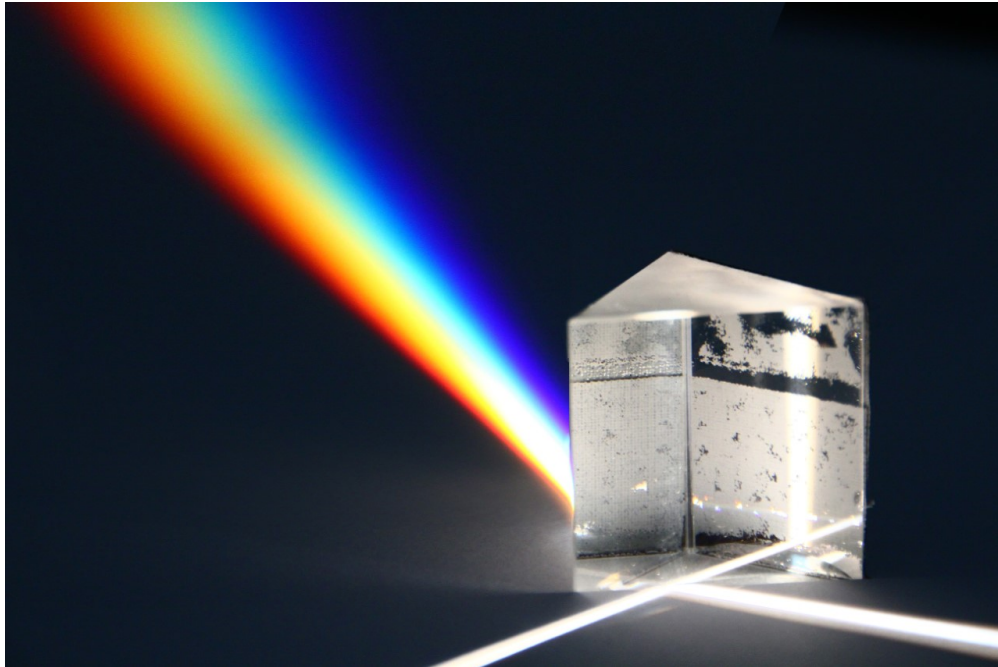


Stellar Spectra and their Analysis with WWW Tools



Introduction and manual

Yannick Pfeifer

Eberhard Karls University of Tübingen
Institute for Astronomy and Astrophysics
Kepler Center for Astro and Particle Physics
Department of Astronomy

February 2017

Cover page:

The image on the cover shows the phenomena of refraction. A beam of white light is refracted into its spectral colours passing through a prism. Many thanks to Werner Schich from the State Seminar for Didactics and Teacher Training in Tübingen, who made this photo possible.

Contents

1	Introduction	1
1.1	German Astrophysical Virtual Observatory	3
2	Spectrum	4
2.1	Refraction caused by a prism	4
2.2	Diffraction through a grating	6
2.3	Continuous spectrum, emission line spectrum and absorption line spectrum	10
2.3.1	Continuous spectrum	10
2.3.2	Absorption line spectrum	11
2.3.3	Emission line spectrum	13
3	Introduction to TMAW	15
4	Absorption lines	17
5	Spectral line broadening	19
5.1	Natural broadening	19
5.2	Pressure broadening/Collisional broadening	19
5.3	Stark effect	20
5.4	Doppler broadening	20
5.5	Rotational broadening	21
6	Representation of spectra	22
7	Determination of parameters with TMAW and TVIS	23
7.1	Effective temperature and line depth	23
7.2	Log g and line wings	25
7.3	Element composition and mass ratio	25
8	Approach of the parameter determination	26
9	Examples	29

9.1	Example A	29
9.2	Example B	32
10	Spectral analysis on the internet	37
10.1	TheoSSA	37
10.2	TMAW	38
10.3	TVIS	39
10.4	TVIS Data Changer	40
10.5	TVIS Interactive	42
11	Spectrometers in school	44
A	Absorption lines quantitative	47
B	Homepages	53
C	Datasets	67
C.1	TMAW Output	67
C.2	TVIS Data Changer Output	68
C.3	Spectra 1 Output	69
D	Declaration to the scientific paper	70

List of Figures

1.1	Electromagnetic spectrum	1
2.1	Newton's prism	4
2.2	Refraction at boundarys	5
2.3	Interference	7
2.4	Double slit qualitative	8
2.5	Double slit quantitatively	9
2.6	Double and mutiple slit	10
2.7	Reflection grating	11
2.8	Differences of spectra	12
2.10	Fraunhofer's record	12
2.9	Planck radiation	13
2.11	High resolution absorption line spectrum of the sun	14
2.12	Coloured flame experiment	14
3.1	Electromagnetic radiation and the atmosphere	16
4.1	Bohr model	17
4.2	Absorption line spectrum of the sun	18
4.3	Observation of Feige 66	18
5.1	Redshift	21
6.1	Rectifikation	22
7.1	TVIS Interactive homepage	23
7.2	Line profiles for different T_{eff}	24
7.3	Line profiles for different T_{eff}	24
7.4	Line profiles for different $\log g$	25
8.1	Comparison of an observation with synthetic spectra	28
9.1	Comparison of Feige 66 with synthetic spectra for $\log g$	29
9.2	Comparison of Feige 66 with synthetic spectra for T_{eff}	30
9.3	Comparison of Feige 66 with synthetic spectra for T_{eff}	30
9.4	Comparison of Feige 66 with synthetic spectra for $\log g$	31

9.5	Comparison of G191-B2B with synthetic spectra for $\log g$	32
9.6	Comparison of G191-B2B with synthetic spectra for T_{eff}	33
9.7	Comparison of G191-B2B with synthetic spectra for $\log g$	33
9.8	Comparison of G191-B2B with synthetic spectra for T_{eff}	34
9.9	Comparison of G191-B2B with synthetic spectra for $\log g$	35
9.10	Parameter determination schematical	36
11.1	Spectrometer from Kvant Ltd. for the use in school	44
A.1	Energy levels of hydrogen	49
A.2	Energy levels and transitions in hydrogen	50
A.3	Grotrian diagram of neutral helium	51
B.1	TheoSSA homepage	53
B.2	Output table of TheoSSA	54
B.3	TheoSSA parameters	54
B.4	Preview function in TheoSSA	55
B.5	TMAW homepage	56
B.6	TMAW input	57
B.7	TMAW request confirmation	58
B.8	List of requested parameters	58
B.9	TVIS interactiv homepage	59
B.10	Saveable image	60
B.11	TVIS hompage	61
B.12	TVIS manual	62
B.13	TVIS commands	62
B.14	TVIS Data Changer	64
B.15	The TVIS Data Changer window	65
B.16	SPECTRA 1 program	66

List of Tables

1	Doppler widths	21
---	----------------	----

1 Introduction

Anyone who has seen a rainbow before could witness that light is not simply light. Its appearance reveals to us the single colour components of white light in a beautiful way. When sunlight passes through little droplets in the air, it gets diffracted in those different colours, which are separated and appear next to each other in a smooth colour shift. A rainbow represents the entire visible spectrum, which is, however, only a small proportion of the electromagnetic spectrum. The human eye is not able to detect the largest portion of the spectrum emitted by the sun. Light has wave properties and can thus be seen as electromagnetic waves, with its colour being determined by the wavelength. The human eye can only trace light of wavelengths between 3800-7800 Angström¹ (Å). Electromagnetic waves can have much longer or shorter wavelengths though. Infrared radiation, for example, is the next major range with longer wavelengths as visible light, whereas ultraviolet is the next major range with a shorter wavelength. Fig 1.1 shows the entirety of the electromagnetic spectrum.

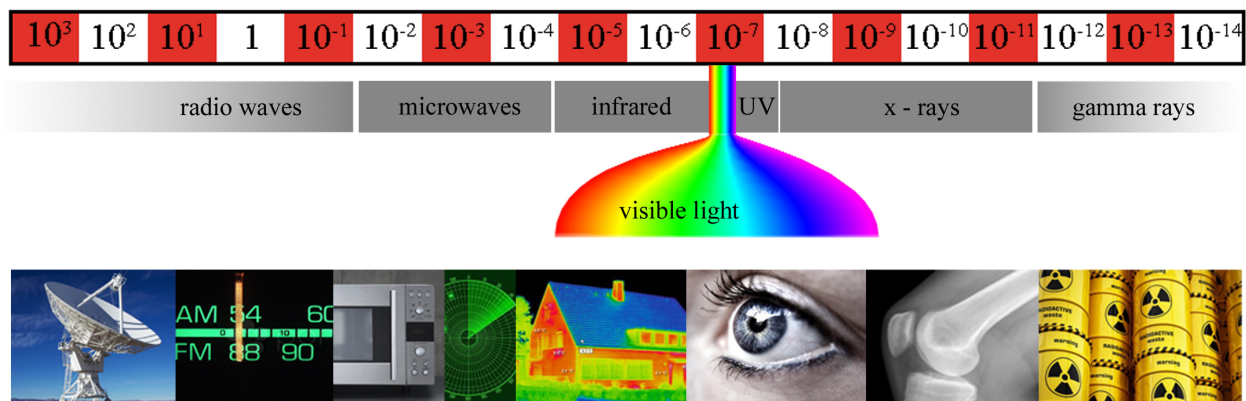


Figure 1.1: Spectrum of electromagnetic waves sorted by wavelengths in [m].

¹1 Å = 10^{-10} m = 0.1 nm

Despite the fact that humans are not able to see wavelengths, which are exceeding the visual range, these can still be detected and measured. As with the light emitted by a light bulb or a glowing piece of iron, the emission of sunlight is caused by the very high temperatures on the sun. The sun is a massive gas ball, which is held together by gravity as a result of its great mass. In its centre, pressure and temperature are so high that nuclear fusion processes are constantly releasing vast amounts of energy. The most important example here is Hydrogen fusion, where four hydrogen atoms with a mass of 1.008 fuse into one helium atoms with a mass of 4.003.



The overall mass of the new Helium atom is 0.029 less than the sum of all four Hydrogen atoms, which it is generated from. According to Einstein, this mass defect of 0.7% (5) is directly converted into energy, following

$$E = mc^2 \quad . \quad (2)$$

c represents the speed of light. This energy is mainly transferred through electromagnetic waves and is radiated in all directions, as soon as it reaches the surface of the sun. The sun emits radiation covering the entire spectrum from the very short to the very long wavelengths. How exactly the corresponding spectrum looks like, depends on the temperature and the surface gravity of the star. Chemical composition does have an influence as well, i.e. elements in the star's atmosphere, which absorb specific wavelengths and thus create spectral lines. Looking at high resolution stellar spectra, differences can be determined and the characteristic radiation of observed stars can reveal information about the parameters mentioned above. This information can then be used to determine, for instance, in which development stage the corresponding star is and to make projections on how it will develop. Such information is critical in order to gain knowledge about how stars come into being and how they develop. After all, this helps us understand the history of the development of the universe.

The following instruction aims to provide an insight into the work with stellar spectra and how information can be gained from such. First, a couple of central phenomena in such spectra are explained. Next, the approach for the determination of parameters of stellar objects will be explained.

Finally, this method will be illustrated by two examples followed by a brief explanation of how the used tools work. There is a practice section on the TVIS Interactive website.

1.1 German Astrophysical Virtual Observatory

The Tübingen Model-Atmosphere World Wide Web Interface (TMAW) is publicly accessible in the course of the German Astrophysical Virtual Observatory² (GAVO). GAVO is the german contribution of the international Virtual Observatory³ (VO) project, which was initiated in order to provide easy large scale access to astrophysical data, as well as to their analysis. As reaction to the ever increasing amount of acquired astrophysical data, this project seeks to simplify access and usage of data. In addition, the VO ensures the optimal use of observation and acquisition resources e.g. by avoiding double observations through prior data base matching. Thus, important observation time can be saved. The Institute for Astronomy and Astrophysics of the Eberhard Karls University Tübingen devotes a part of its work to this project.

²<http://www.g-vo.org>

³<http://www.ivoa.net>

2 Spectrum

2.1 Refraction caused by a prism

Initially, there is the question, how incident light can be split up in such a way, that its spectral distribution becomes visible. In the 1770's the English scientist Sir Isaac Newton was the first one to realise that white light is actually made up of light of all colours. On his search for an explanation of the properties of light, he guided a beam of sunlight through a small pinhole onto a prism. On a screen on the opposite side, he saw what he would henceforth call a colour spectrum (3). Fig. 2.1 shows the setup of his experiment.



Figure 2.1: Isaac Newton and his apparatus for refracting white light in the spectral colours.
Source: <http://www.escuelapedia.com/el-arco-iris/>, 26.1.2017

However, Newton was not able to find an explanation for this phenomena. Although improved in many quality aspects, the use of prisms is still a fundamental method to split light beams in their spectral colours today. The method is based on the principle of refraction of a light beam at the boundary between an optically thick (high refractive index) and optically thin (low refractive index) medium.

When an incident ray, passing through air (low n), meets the surface of an optically thick medium

(e.g. glass, high n), at an angle other than the normal of the boundary surface, it will be refracted towards the normal. When the incident light is in the optically thick medium before it hits the boundary, it will be refracted away from the normal. This can be explained by Huygens' law, which states that every point of a wave front can be seen as the source of a spherical wave. Fig.2.2 shows the principle.

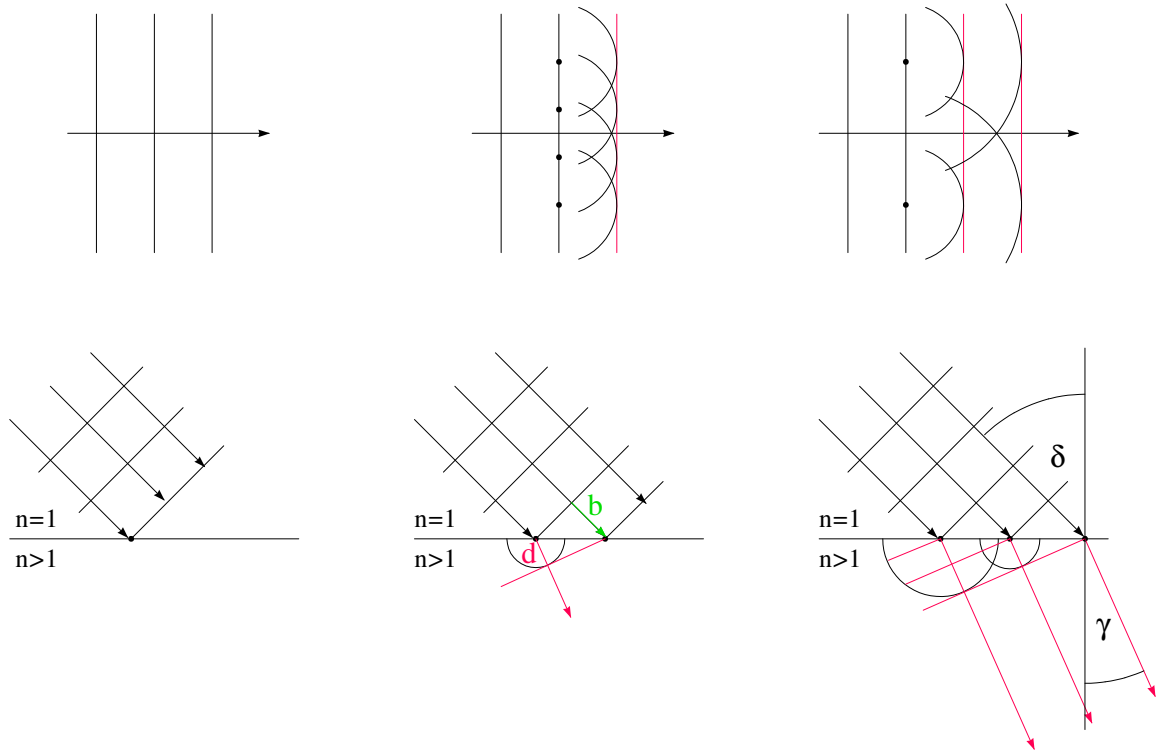


Figure 2.2: Above: New wave-fronts made up by secondary waves following Huygens law. Below: Propagation of wave-fronts through a boundary between two mediums with different refractive indices.

As said previously, light can be described with wave properties. This principle applies in air, as it does in other mediums, for instance glass. However, it is noteworthy, that the propagation speed c_n in the medium is slowed down in relation to the refractive index n , compared to the propagation speed in vacuum c . The following equation applies:

$$c_n = \frac{c}{n} \quad . \quad (3)$$

This causes a change in the propagation direction, as shown in fig. 2.2. The incident light reaches the boundary step by step under the incident angle δ . As one part of the wave front already propagates

in the optically thicker medium, the other part has yet to reach the boundary surface. However, in the optically thicker medium, the propagation speed is slower, thus, the part of the wave front, that hit the boundary first, has propagated the distance d . In the same time, the distance b has been traveled by the part of the wave front that reaches the boundary last. If a new wave front is constructed from the spheric waves in the medium, it becomes clear that the refracted rays have changed their direction of travel towards the normal of the boundary surface and are now propagating under the angle of refraction γ . This explains the refraction, however, it does not explain the separation of colours. This is caused by the wavelength-dependency of the refractive index,

$$n = n(\lambda) \quad . \quad (4)$$

An increasing wavelength in the incident ray corresponds with a decreasing refractive index. This means that red light will be refracted less than blue light, which causes the spacial separation.

2.2 Diffraction through a grating

A more versatile and thus more common possibility of separating the colours of a light beam is the use of a diffraction grating. Huygens' law plays an important role here as well. Moreover, the principle of superposition plays a crucial role as well, another consequence of the wave properties of light. Fig. 2.3 shows two waves of similar wavelength. They can be superposed in such ways, that they either superpose constructively or destructively. In order to get constructive superposition (interference), the waves have to be in phase, which means that their displacement peaks are lined up over one another and in the same direction. In order to get destructive interference, the waves have to be in antiphase, meaning the displacements in opposite direction are lined up over one another. They will then cancel out each other.

If light is irradiated on a double slit as illustrated in fig. 2.4, each of the slits will act as a source of spheric waves (Huygens' principle). These spheric waves superpose on the other side of the slit. The red arrows indicate the directions of constructive interference (where the circles intersect).

Where exactly they will superpose constructively and destructively, can easily be determined quantitatively through fig. 2.5. For constructive interference, the displacement peaks in the same

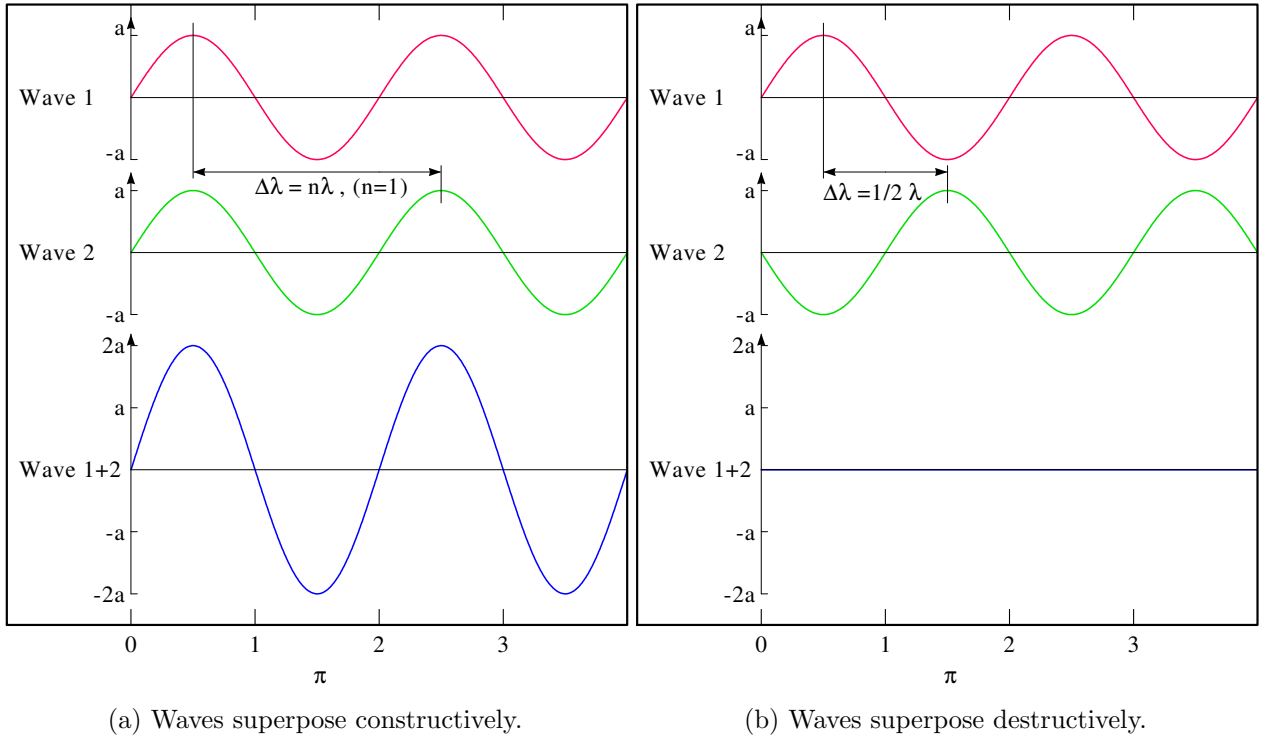


Figure 2.3: Superposing waves.

direction have to line up. This happens when they are in phase or shifted against each other by an even multiple. This is the case, if we look at a propagation direction different to the normal of the slit screen. If the propagation angle relative to the normal is such, that it causes a path difference between the two spheric waves which is once or an even multiple of the wavelength, constructive superposition will occur.

Mathematically this interference condition, the Bragg condition, (in accordance with fig. 2.5) is expressed as

$$\sin \alpha = \frac{\Delta \lambda}{d} = \frac{n \lambda}{d} \quad . \quad (5)$$

For small angles $\alpha < 5^\circ$,

$$\sin \alpha \approx \alpha \quad (6)$$

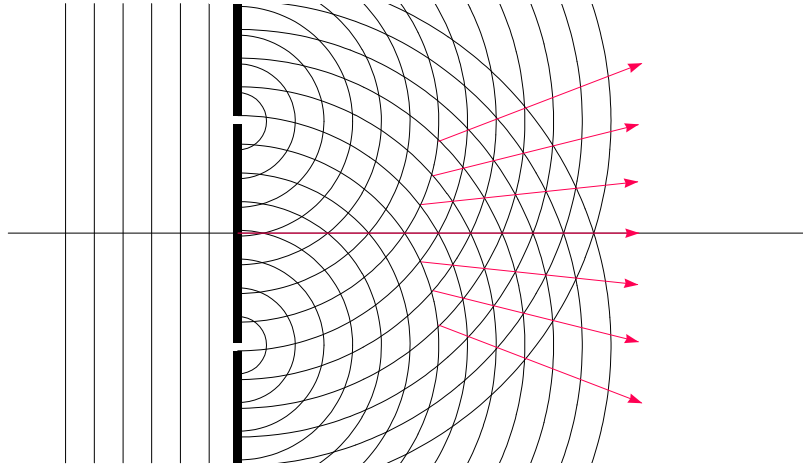


Figure 2.4: Double slit with incident light and resultant spheric waves and superposition.

applies, which simplifies Eq. 5 to

$$\alpha = \frac{n\lambda}{d} . \quad (7)$$

The condition for destructive interference can be formulated analogous as

$$\sin \alpha = \left(n - \frac{1}{2} \right) \lambda = \left(2n - 1 \right) \frac{\lambda}{2} , \quad (8)$$

which is also simplified for small angles to

$$\alpha \approx \left(2n - 1 \right) \frac{\lambda}{2} . \quad (9)$$

Here n is a natural number and specifies the path difference between the two waves as a multiple of wavelengths. The result is an intensity distribution in dependency of the propagation angle as depicted in fig. 2.6 ($N = 2$, here N designates the number of slits). As opposed to refraction, this change of propagation direction is called diffraction. The position of the intensity maximums is described by Eq. 7, that of minimums by Eq. 9.

So far, this examination has only taken into account monochromatic (single-coloured) light. What happens when polychromatic light passes a double slit is clear from Eq. 7. Depending on the

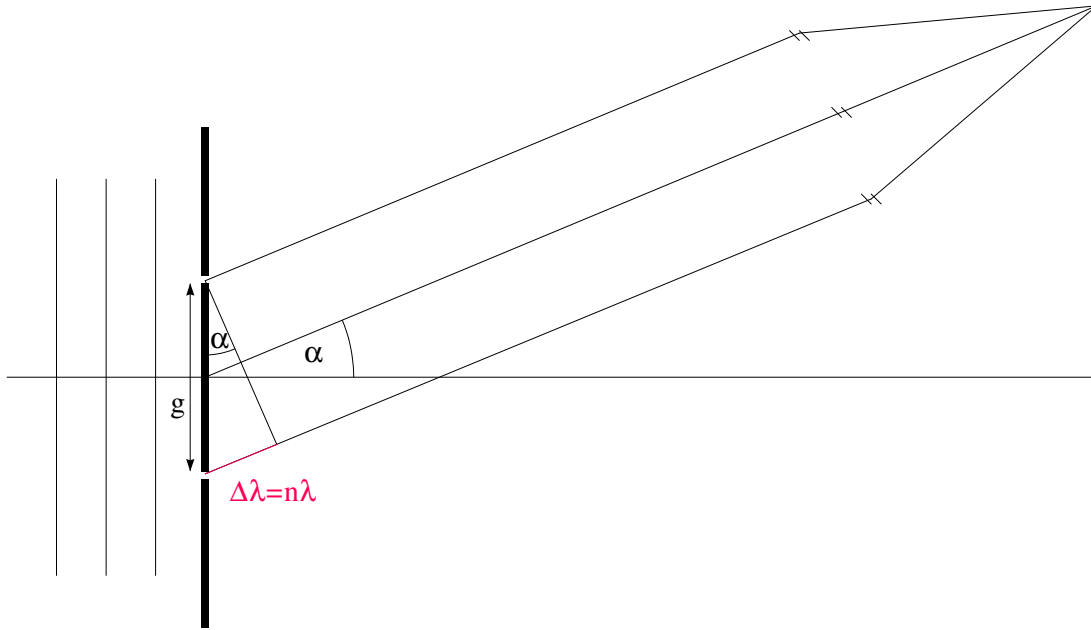


Figure 2.5: Scheme of a double slit with width g .

wavelength of the light contained in the beam, different coloured maximums will result under different diffraction angles. Fig. 2.6 ($N=2$) illustrates that a maximum produced by a double slit is stretched over a certain spacial range. If two colours with only a slight difference in wavelength are diffracted, their maximums will overlap and the colours will merge. In order to achieve very sharp maximums, many more slits can be added to the double slit, eventually creating a grating. For N slits there are $N-1$ minor maximums inbetween the major maximums, which become increasingly sharper. Fig. 2.6 illustrates this tendency.

For detailed analyses of spectra, it is of great importance to separate spectral colours as good as possible. Or to put it differently: The diffraction angle must be as big as possible and with it the resolving power of the spectrum. It is clear from Eq. 7, that this can be achieved by significantly reducing the distance g between the slits. The smaller this grating constant is, the clearer the spectral separation will be. Furthermore, a diffraction grating can not only be realised as a permissive grating, but also as a reflective grating as shown in fig. 2.7. The position of maximums shall not be discussed here.

At a reflection grating, the path difference is no longer caused by equidistant slits, but by regular steps on a reflective surface. The advantage of this realisation is its compact structure and its high light yield, since 50 % of the incident light is not blocked by the grating anymore. This makes

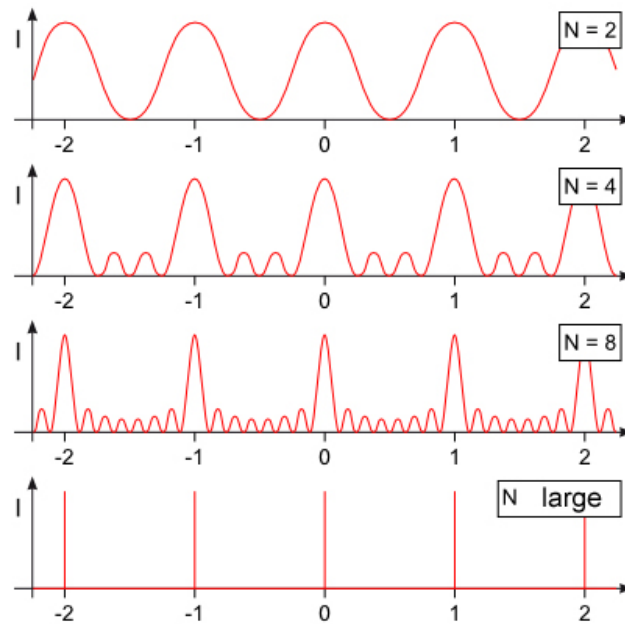


Figure 2.6: Diffraction pattern for $N=2, 4, 8$ and many slits.
 In the style of: <https://lp.uni-goettingen.de/get/text/1055> 11.1.2017

the observation of stars with low luminosity feasible. An apparatus for separation of light into its spectral colours is called spectrograph. If it can analyse the spectrum regarding wavelength and intensity, it is called a spektrometer.

2.3 Continuous spectrum, emission line spectrum and absorption line spectrum

Depending on what a spectrograph is pointed at, different spectra can be observed. Those can be categorised as continuous spectra, emission line spectra and absorption line spectra. Fig. 2.8 illustrates the differences.

2.3.1 Continuous spectrum

If a spectrograph is pointed at a regular light bulb, a continuous spectrum will be the observed. In 1900, Max Planck was the first one to successfully explain the radiation behaviour of hot bodies. Those emit a continuous spectrum, the maximum of which is shifted in dependency of the temperature as illustrated in fig. 2.9. This is why metal glows in different colours depending on the temperature.

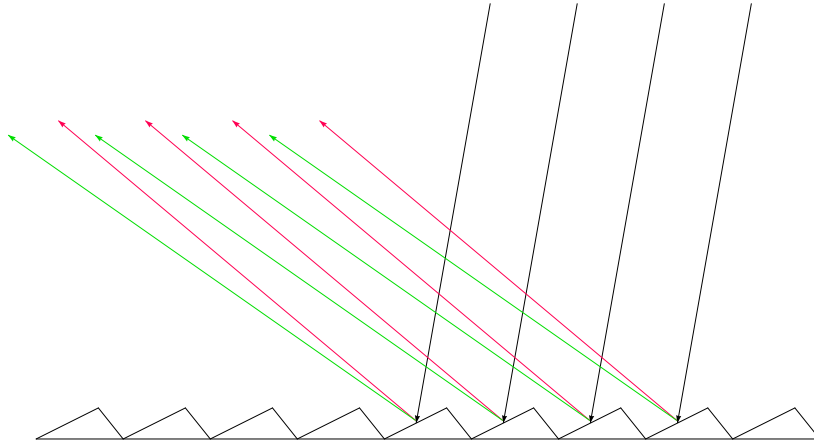


Figure 2.7: Scheme of a reflection grating.

2.3.2 Absorption line spectrum

When a gas is placed between light source and spectrograph, the result will be a absorption line spectrum. It looks almost like a continuous spectrum (which is what is emitted by the light source), but is defined by a few missing wavelengths, which are characteristic for the gas (fig. 2.8). Those wavelengths have been absorbed by the gas between light source and spectrograph and have vanished from the spectrum. They show as black lines. An absorption line spectrum is recorded, which is like a unique fingerprint for every gas.

The same result can be seen, when a spectrograph is pointed at the sun. In this case, however, there are significantly more absorption lines. Fig. 2.10 shows the record of Joseph von Fraunhofer (1787-1826), who was the first one to detect these lines in the sun's spectrum, which is why they are named after him. The curve, which was later to be successfully described by Planck, is already sketched qualitatively. The number of absorption lines hints at a number of different elements.

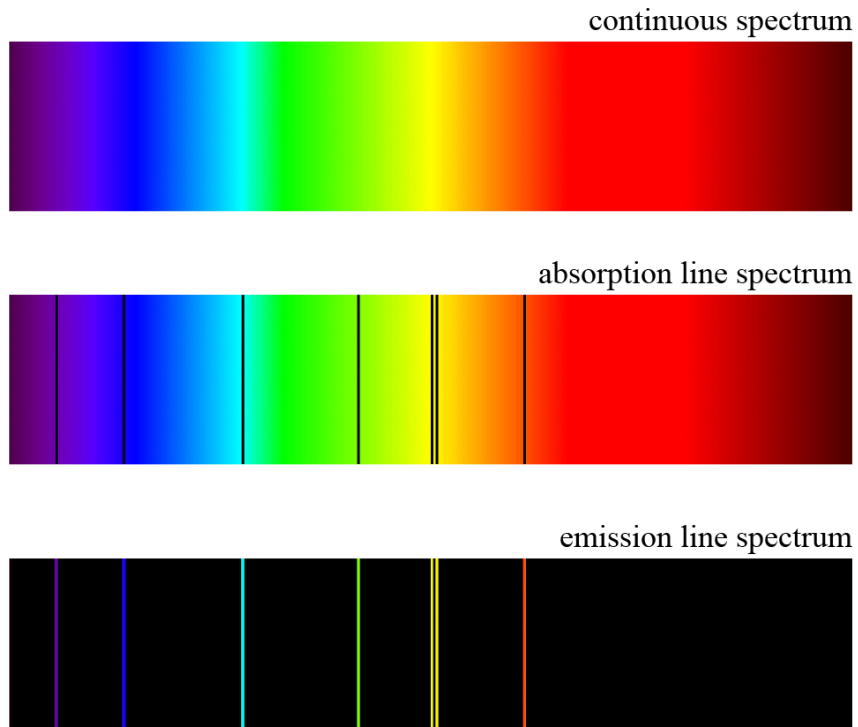


Figure 2.8: Continuous spectrum, emission line spectrum and absorption line spectrum of mercury.

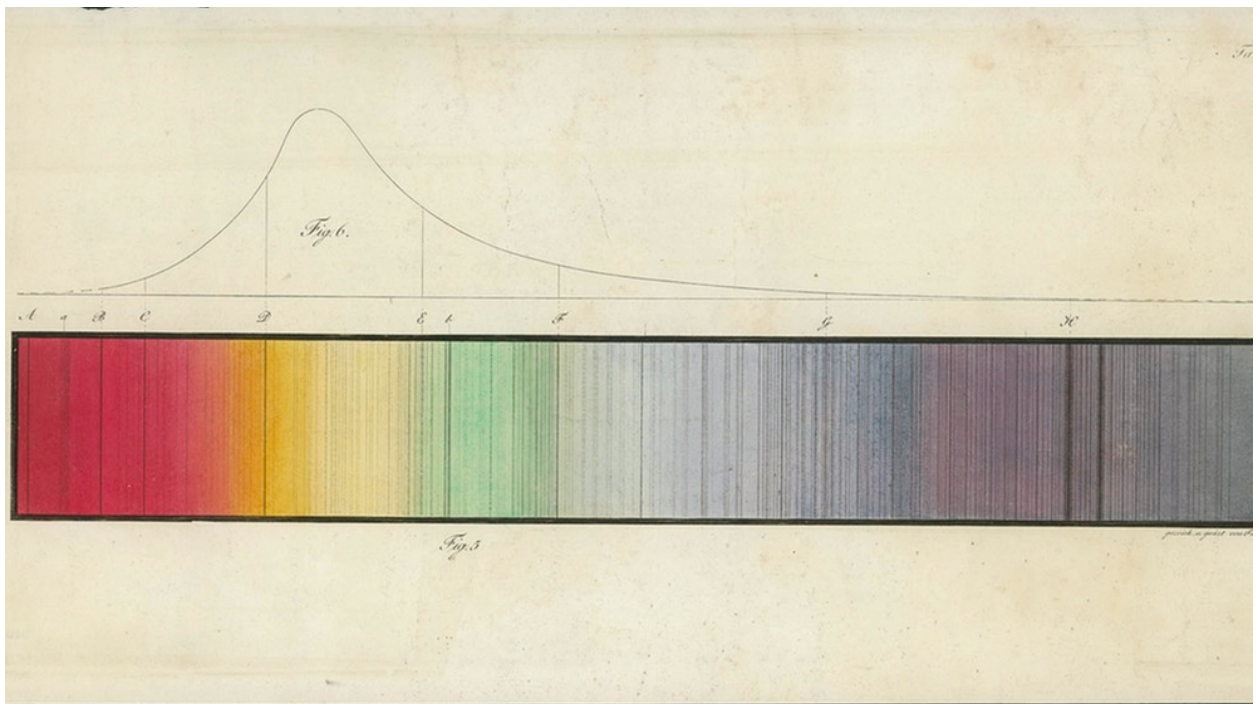


Figure 2.10: Fraunhofer's record in the *Deutsches Museum*.

Source: <http://www.br.de/themen/wissen/fraunhofer-spektrallinien102.html>, 14.12.16

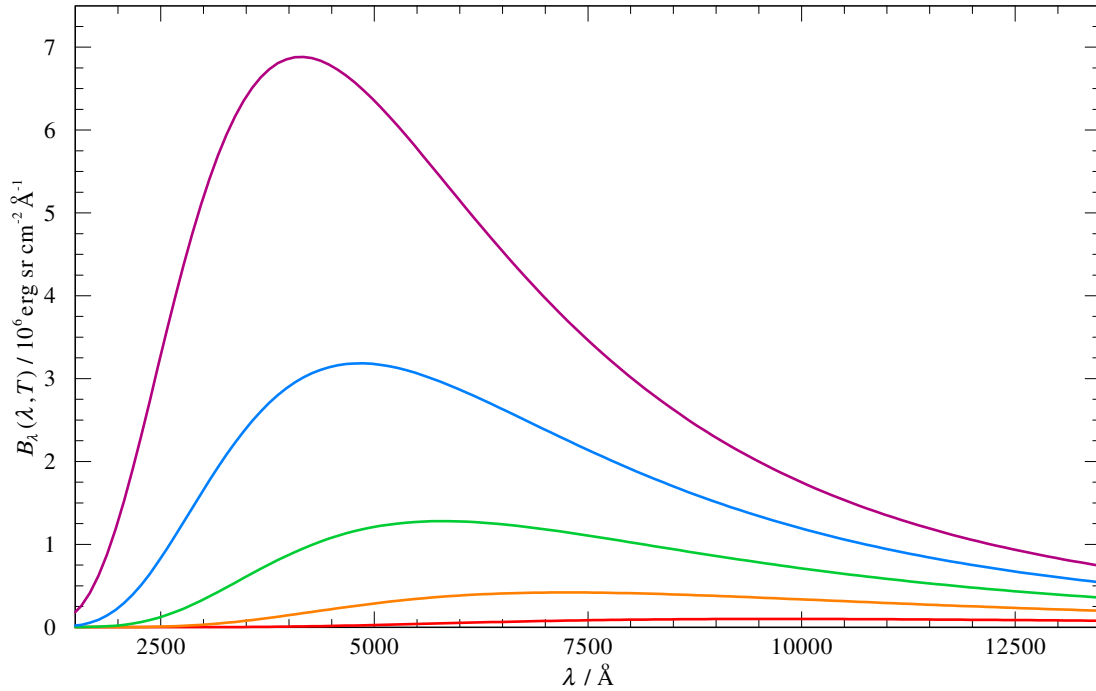


Figure 2.9: Planck radiation behaviour of a hot body. $T = 7\,000\text{ K}$ (purple), $T = 6\,000\text{ K}$ (blue), $T = 5\,000\text{ K}$ (green), $T = 4\,000\text{ K}$ (orange), $T = 3\,000\text{ K}$ (red).

Nowadays, the spectrum of the sun can be recorded with much higher resolution, which is shown in fig. 2.11. A great number absorption lines can be seen.

2.3.3 Emission line spectrum

If we switch of the light source and heat up the same gas long enough to make it glow, there will only be a few colours in the spectrum. Those are visible at the same positions where the lines are in the absorption line spectrum (fig. 2.8). Since they form from emission, the resulting spectrum is called emission line spectrum.

In school, this phenomena kann be used to determine which element was burnt by looking at the colour of the flame. If for example, sodium is placed in a flame, it is heated up until it starts burning in a colour, which is characteristic for sodium. Thus, based on the colour and the resulting emission line spectrum, it is possible to determine, which element was burnt. Fig. 2.12 a) and b) show six flames of different elements being burnt with the corresponding emission line spectra.

The cause of emission and absorption line spectra will be discussed more thoroughly in chapter 4.

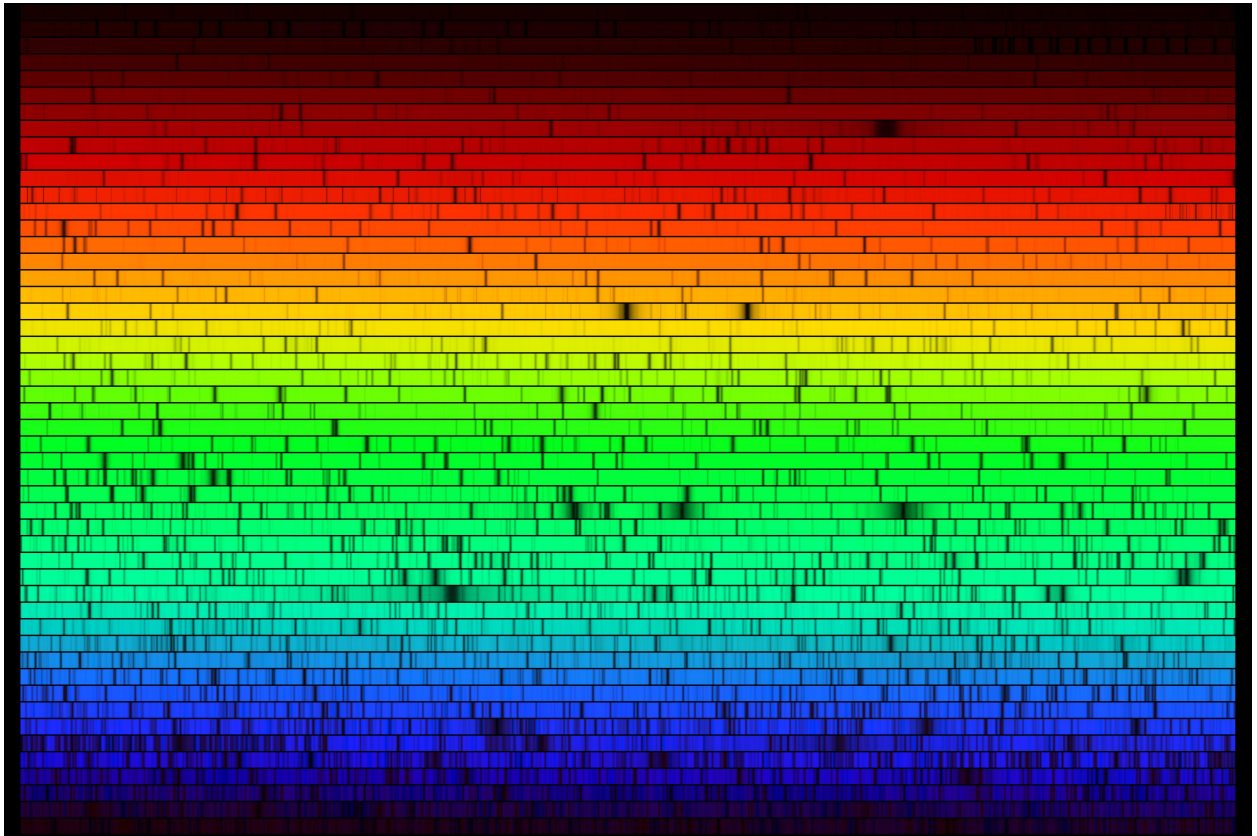
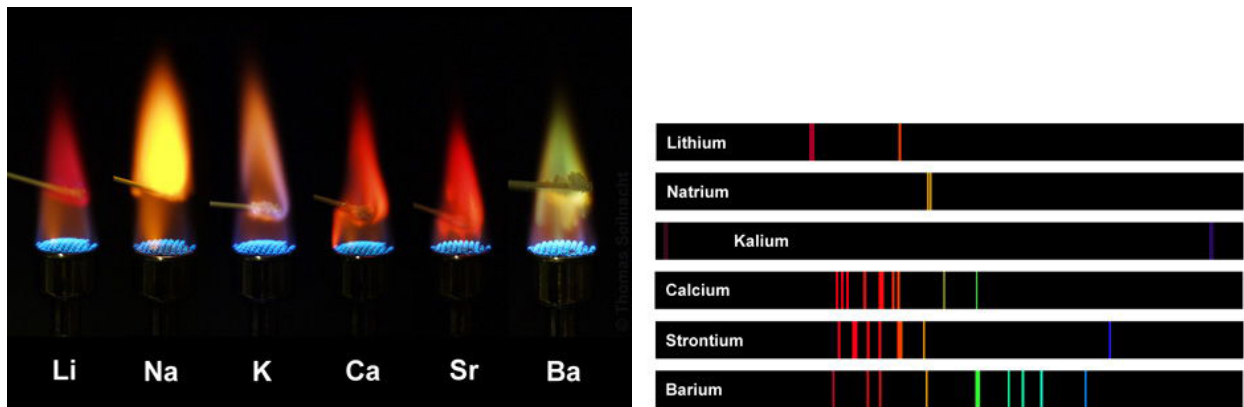


Figure 2.11: Spectrum of the sun recorded by the National Solar Observatory on Kitt Peak in Arizona, USA.

Source: https://www.noao.edu/image_gallery/html/im0600.html, 21.12.16



(a) Flames at the burning of different elements.

(b) Corresponding emission line spectra.

Figure 2.12: Coloured flames and the corresponding emission line spectra of the elements Li, Na, K, Ca, Sr und Ba.

Source: <http://www.seilnacht.com/versuche/spektro.html>, 6.2.2017

3 Introduction to TMAW

TMAW is a tool for calculations of stellar model atmospheres. It serves as aid for international researchers and amateurs alike, to determine the important parameters of observed objects. Surface gravity, effective temperature and chemical composition are the parameters, which specify a model atmosphere in TMAW. The basis for this kind of research are stellar absorption line spectra, as the only source of information about these objects. The user determines the variables by carefully comparing the recorded spectrum with the spectra of the calculated model atmospheres. By gradually changing the parameters, the greatest possible match can be achieved in the most prominent wave length ranges. Especially for scientific purposes, it is desirable to work with spectra, which cover a broad range from the far ultraviolet to the infrared light, in order to perform a thorough and detailed analysis. Since there will only be ground-based telescopes available for school and amateur astronomers, this analysis will be limited to the visual range of the electromagnetic spectrum. A great part of the spectrum outside the visual range is blocked by the earth's atmosphere, which limits the examination of spectra. The ultraviolet waves are absorbed. A small part of the radio waves is reflected, the largest proportion, however, passes the atmosphere, which is why radiotelescopes can be used to observe the universe. These circumstances are the most decisive factors for the development of space telescopes. Fig. 3.1 shows which parts of the electromagnetic spectrum are absorbed by the earth's atmosphere and which parts reach it's surface.

The synthetic spectra are calculated by TMAW on the basis of the known physical processes in stars. The calculation of model atmospheres is based on extensive and constantly improved atomic datasets, which contain detailed information about ionisation stages, atomic levels and their transitions, as well as the corresponding transition probabilities. Key components of the calculation are the highly non-linear systems of equation for the parameters (i.e. population density, line transitions, charge conservation etc.) of the radiation transport equation. Calculations are very time consuming and usually have to be solved in a couple of thousand iteration cycles. Additionally, there are statistical equations and side conditions which have to be considered.

A star's atmosphere can not be determined as easily as the earth's. What is actually meant is a star's photosphere, which is the outer layer, in which photons from the star's inside can pass outside without obstruction (otherwise we couldn't see them). It is assumed that a continuous spectrum is

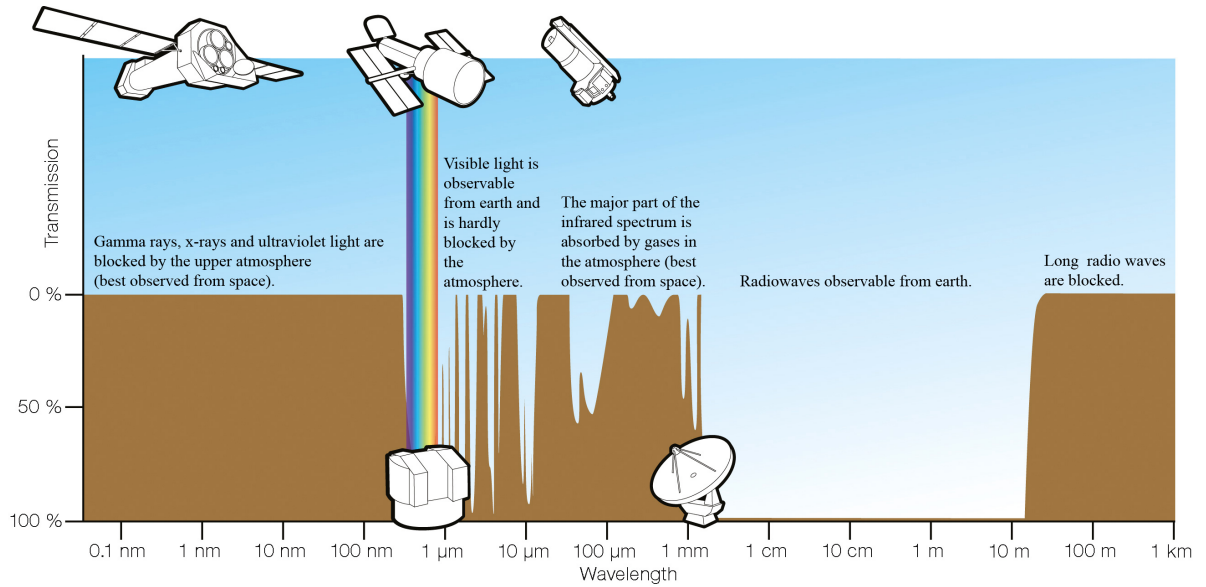


Figure 3.1: Atmospheric opacity for electromagnetic waves.

In the style of: https://www.eso.org/public/germany/images/atm_opacity, 12.12.2016

incident to the photosphere from below, due to nuclear fusion within the star. In the photosphere, there are different elements that absorb specific wavelengths of the outgoing electromagnetic spectrum. Thus, the spectrum of the star is not a continuum anymore, but an absorption line spectrum in accordance with the star's specific parameters.

4 Absorption lines

In order to understand the cause of absorption lines in stellar spectra, we can consider Bohr's classical model of the atom. Key element of his model was the assumption that electrons cannot move in any random distance to the atoms core. Bohr postulated that there must be different discrete circular orbits on which electrons could move.

Electrons can change to a larger circular orbit of higher energy through the external input of energy in the form of light, as illustrated in fig. 4.1. The arrows represent potential transitions to circular orbits with higher energy levels.

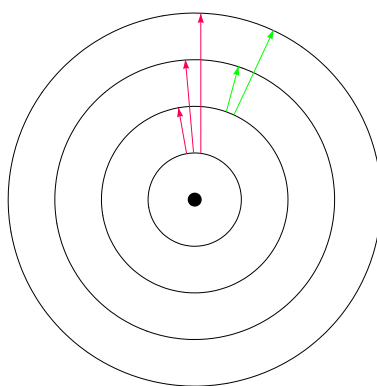


Figure 4.1: Bohr model atom.

For such a transition, a clearly defined amount of energy is necessary. Thus, exactly those wavelengths of the incident light are absorbed, which can be attributed to such defined energy amount. Those can easily be determined, following Planck with

$$E = h\nu = \frac{hc}{\lambda}; \quad \lambda = \frac{hc}{E} \quad . \quad (10)$$

h is Planck's constant ($h=6.62610^{-34}$ Js), ν the frequency of the electromagnetic radiation, E the energy, c the speed of light and λ the corresponding wavelength. That way, every transition in an element absorbs (and emits when applicable) light of a characteristic wavelength.

If the spectrum of a stellar object is recorded with a spectroscope, it simply records the intensity of the light (radiation flux) in dependence of the respective wavelength λ . The position in the spectrum, which corresponds with the wavelength of the absorbed light, shows a dark line. Significantly less or

no light of that wavelength was recorded.

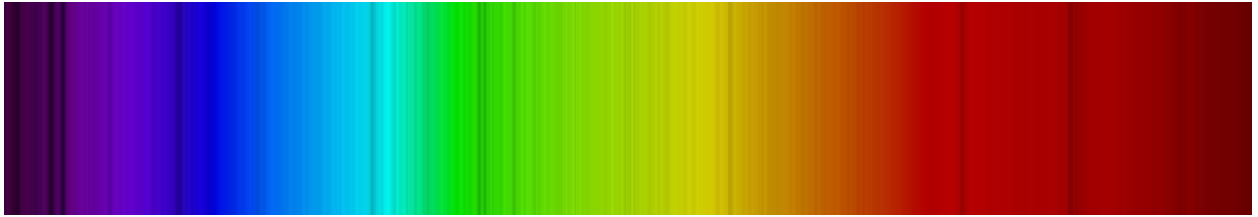


Figure 4.2: Absorption line spectrum of the sun in the visual range.

Source: <http://ganymede.nmsu.edu/tharriso/ast110/class13.html>, 11.12.2016

The dark lines are clearly visible in fig. 4.2. With the development of CCD (Charge Coupled Device) detectors the analysis of spectra has become a lot easier and better. The spectrum is projected on a sensor, the pixels of which detect the impact of single photons of the projected colour. This allows the measurement of intensity in addition to the position. In a spectral energy distribution, the countrates of the CCDs are plotted against the wavelength, as shown in fig. 4.3. This allows very precise analyses of astronomical spectra. Astronomers generally work with high resolution spectra in order to achieve relevant results, which can be seen by the fact that it is common to provide electromagnetic wavelengths in \AA ($=0.1 \text{ nm}$) and not in nanometers. However, the resolution, which is the ability to distinguish two closely positioned points of light, depends on the spectrograph.

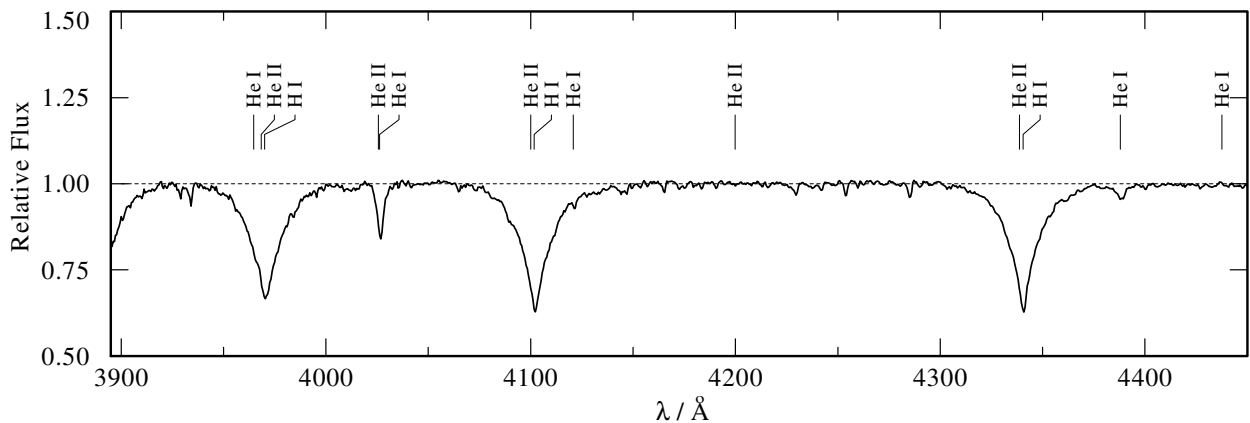


Figure 4.3: Observed spectrum of the star Feige 66. The dashed line represents the continuum flux.

5 Spectral line broadening

As previously mentioned, in the atom model after Bohr, there are clearly defined energy levels, between which radiative transitions can take place. The discrete amounts of energy, required to perform such a transition, are provided by photons in this context. Those can be related to a wavelength. Thus, we would expect sharp lines of absorbed wavelengths, when looking at a spectral energy distribution. However, spectral energy distributions show that the absorption lines are broadened over a small wavelength intervall towards both sides of the center of the absorption lines. There are a couple of effects which cause that phenomena, so called line broadening mechanisms. Which different effects have to be taken into account when discussing line broadening mechanisms, and how great their respective influence is, shall be discussed in this chapter.

5.1 Natural broadening

The spontaneous de-excitation of higher energy levels to lower levels limits the possible life span of excited states, which is therefore subject to a statistical distribution. According to Werner Heisenberg's (1901 - 1976) principle of uncertainty between energy and time,

$$\Delta E \cdot \Delta t \geq \frac{\hbar}{2} \quad , \quad (11)$$

this uncertainty in life span causes an uncertainty in the energy levels of the atom. It is referred to as natural broadening, since this effect is relevant, even if the particle is not influenced by others.

Influence:

Natural broadening is dependent on wavelength and is in the scale of a few femtometers (10^{-5} Å).

5.2 Pressure broadening/Collisional broadening

Due to constant collisions with other particles, atoms reach a kind of state of vibration, which causes the energy levels to blur. The higher the pressure, the more collisions occur during a set time interval. Therefore, the magnitude of the vibration increases, and with it the shift of energy levels.

Influence:

Pressure broadening is dependent on wavelength as well. It is in the scale of a couple of 10 femtometers (10^{-4} Å).

5.3 Stark effect

The presence of other particles with electric charge in the immediate proximity of the respective atom causes a distortion of the electrostatic field. This in turn causes a shift in the energy levels and a change in level transitions. Protons and electrons have the biggest influence as disruptive particles. This effect is referred to as Stark effect (Johannes Stark, 1874-1957).

Influence:

In strong fields, the Stark effect can influence line profiles across many 100 Å.

5.4 Doppler broadening

Generally, particles that absorb photons are not static, they move. Every particle has a movement component relative to the line of sight of the observer. Photons, which reach the observer on earth, travel exactly on this line of sight. Absorbing atoms will, depending on the direction of movement as well as the velocity, perceive the wavelengths of those photons differently, following

$$\frac{\Delta\lambda}{\lambda} = \frac{v}{c} \quad . \quad (12)$$

Fig. 5.1 illustrates the principle: 1.) represents the lines, which are usually absorbed when static. If an atom moves towards the light source, the wavelength of the photons will be perceived as shorter. The spectrum will be perceived as blueshifted (2.)). This blueshift has the consequence, that the atoms will absorb those wavelengths of the shifted spectrum that they usually absorb (3.)). For the static observer on earth, however, the spectrum has not shifted, but the absorption lines now appear redshifted (4.). While the spectrum for the absorbing atoms is blueshifted, the corresponding absorption lines are redshifted. The blueshift of absorption lines with opposite movement can be explained analogous.

Thus, photons can be absorbed, which can be attributed to wavelengths that are a little shifted in comparison the original wavelength required for a line transition. The broadening of the absorption

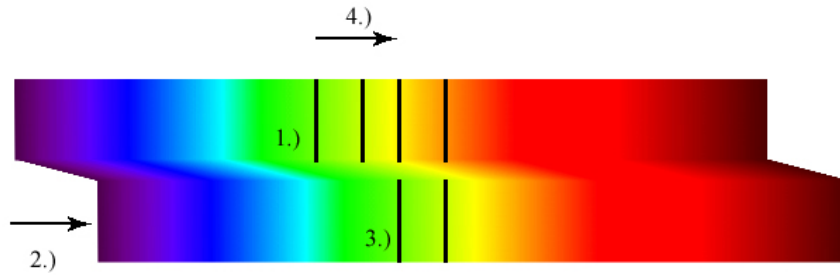


Figure 5.1: Redshift principle.

line is fundamentally determined by Maxwell's distribution of velocity for the absorbing particles.

Influence:

Doppler broadening influences line profiles in the scale of 0-3 Å (Tab.1).

Table 1: Doppler widths for lines with wavelengths 250 Å, 2500 Å and 25000 Å for the elements H, He, C, N, O at $T=100\,000\text{ K}$.

Element	250 Å	2500 Å	25000 Å
H	0.033	0.338	3.387
He	0.016	0.169	1.693
C	0.009	0.097	0.977
N	0.009	0.090	0.905
O	0.008	0.084	0.844

5.5 Rotational broadening

In addition to thermal Doppler broadening, lines can be shifted as a result of the rotation of a star as well. The fundamental principle of Doppler broadening applies here too. In this case, the different relative wavelengths are caused by the fact that one half of the star constantly moves towards the observer, whereas the other half moves away from them.

Influence:

In extreme cases, rotational broadening can stretch absorption lines to such extent, that they are recorded as broad troughs.

6 Representation of spectra

This chapter will briefly deal with the representation of spectra. So far, only normalised spectra have been depicted in this thesis. Those are spectra where the relative flux is plotted instead of the absolute flux. They are normalised against the flux of the continuum without spectral lines. If a continuum was normalised, it would simply show as a horizontal line at 1.0. A normalised representation is clearer and the examination of lines a lot easier. These spectra are also called rectified. Fig 6.1 shows both representations in order to highlight the differences.

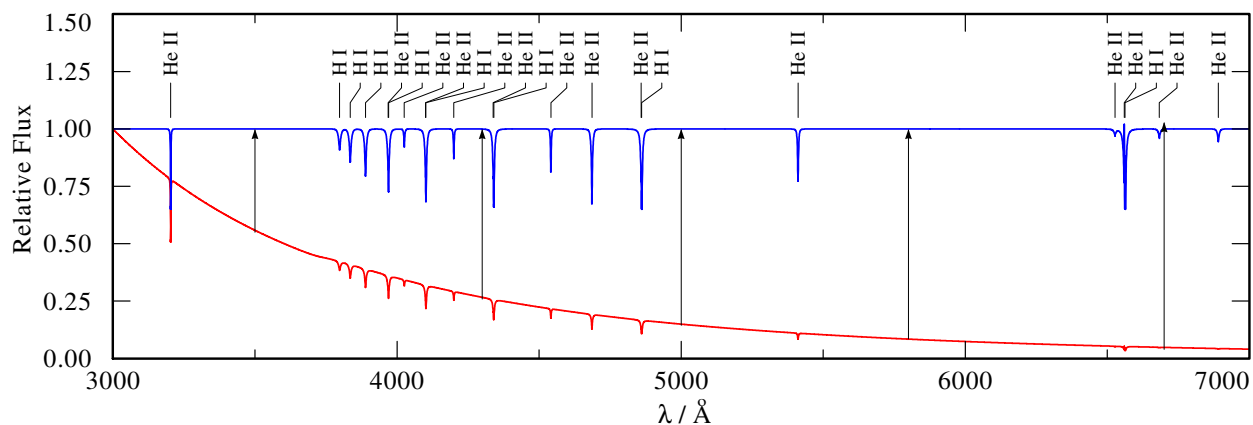


Figure 6.1: Model spectra. Absolute (red) and rectified (blue) flux. H- and He-lines are indicated.

The model spectra in the TMAP database can be normalised or non-normalised. Observation data are commonly rectified, but can be non-normalised as well. Therefore it is important to make sure that both observation and synthetic spectra are in the same mode of representation in order to ensure a proper analysis.

7 Determination of parameters with TMAW and TVIS

How the development of absorption lines and their broadening is linked to stellar parameters such as temperature, surface gravity and chemical composition, is programmed in TMAW. The user only has to specify those values and compare the synthetic spectra with the observation. In order to simplify the analysis of spectra, the Institute for Astronomy and Astrophysics of the University of Tübingen has published the TVIS Interactive tool. TVIS and TVIS Interactive have been developed by Denny Hoyer. This process was supported in the course of this thesis. It enables the user to plot data easily and intuitively, without having to become acquainted with a plotting program first. That way, preliminary analyses can be completed quickly and without any problems. Fig. 7.1 shows the TVIS Interactive homepage during the analysis of a spectrum. How spectra react on variations of key parameters, will be explained in this chapter. The TVIS Interactive functions will be explained thoroughly in chapter 10.5.

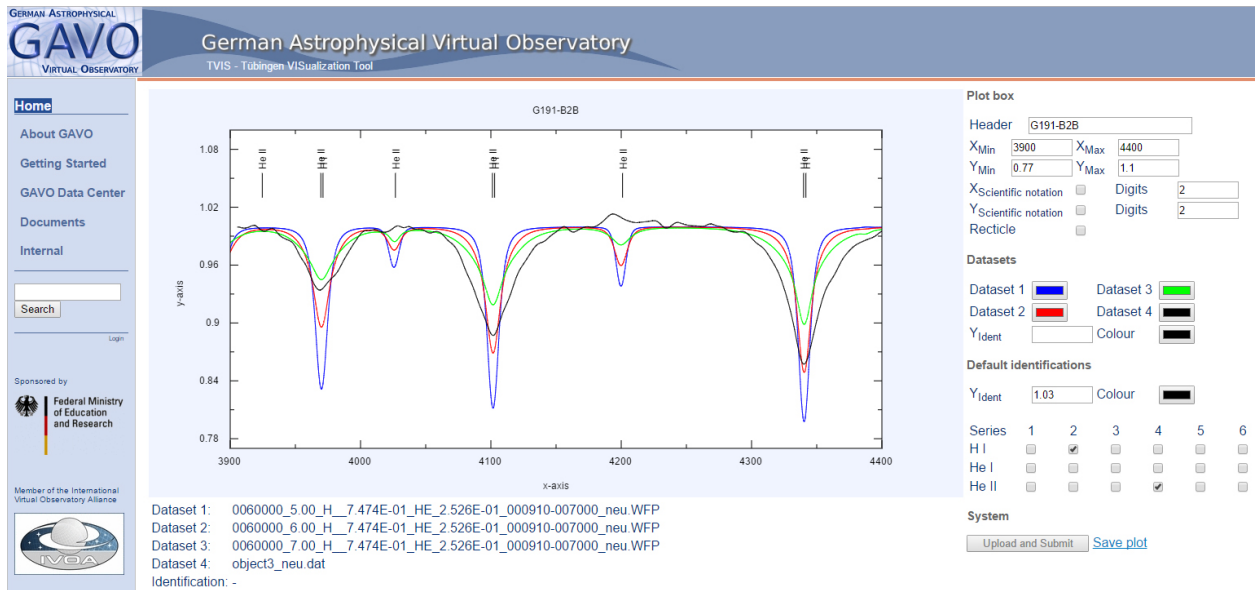


Figure 7.1: The TVIS Interactive user interface during the comparison of three synthetic spectra with an observation.

Source: <http://astro.uni-tuebingen.de/~TVIS/> 3.2.2017

7.1 Effective temperature and line depth

A change in effective temperature (T_{eff} in K) of a model with set surface gravity ($\log g$ in $\frac{\text{cm}}{\text{s}^2}$) will primarily result in a change of depth of the central depression of the absorption line. The line width

however, hardly changes as long as

$$\frac{\Delta T_{\text{eff}}}{T_{\text{eff}}} \ll 1 \quad (13)$$

is valid. Generally, the absorption line will almost keep the same width, even though it is only very weak in the outer wings. Fig. 7.2 and fig. 7.3 show such developments.

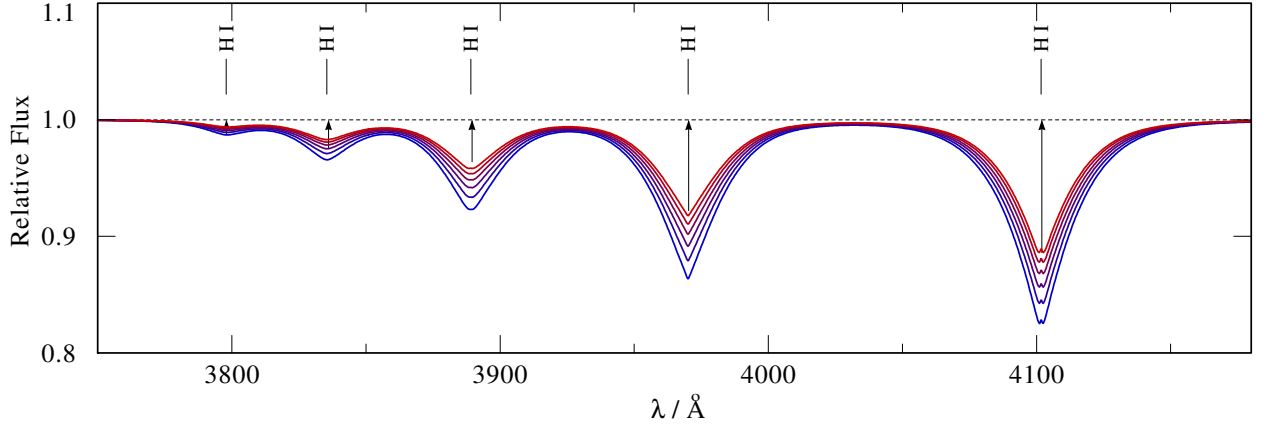


Figure 7.2: Line profiles for $T_{\text{eff}} = 55000$ K (blue) up to 80000 K (red), in steps of 5000 K.

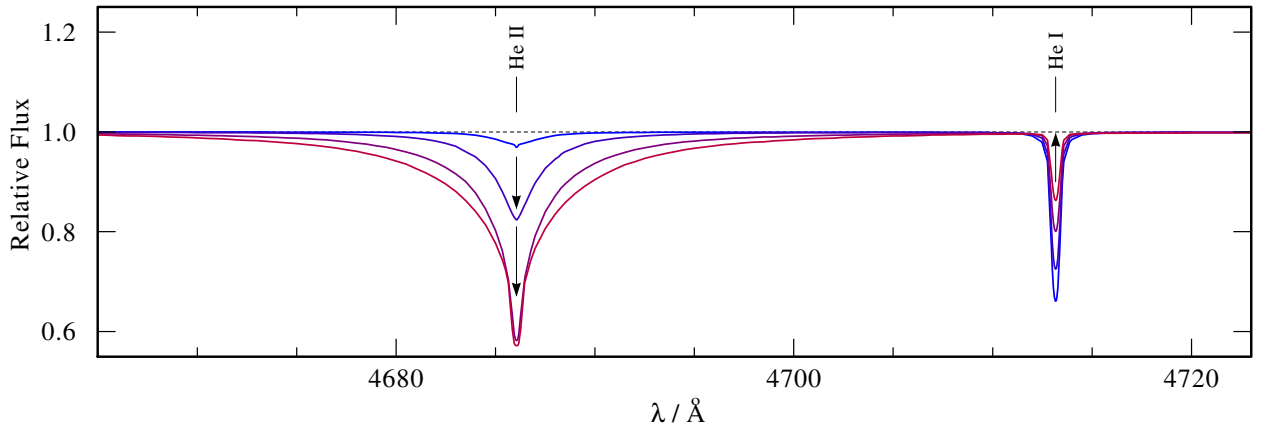


Figure 7.3: Line profiles for $T_{\text{eff}} = 30000$ K (blue) up to 45000 K (red) for lines of different ionisation stages.

Depending on which line is currently examined, an increase of temperature can either result in a stronger or a weaker absorption line. These contrary developments can be explained as follows. With a continuous increase of T_{eff} , more electrons are constantly excited to a higher energy level, as the total energy increases. Therefore, there are more photons absorbed for this specific transition, the absorption line gets stronger.

If T_{eff} is increased further, a threshold will be reached, at which some atoms will reach a higher ionisation stage. Their electron configuration changes and as a result, new absorption lines will show, as explained in chapter 4. Consequently, absorption lines which can be attributed to lower ionisation stages get weaker, as there are now less atoms of that ionisation stage. Thus, an ionisation equilibrium between different ionisation stages (e.g. He I and He II in fig. 7.3) will develop, depending on the total energy. If T_{eff} increases further, more atoms will have the higher ionisation stage and the respective absorptions lines will get stronger. This way absorption lines can get weaker with increasing temperature as well.

7.2 Log g and line wings

A change in $\log g$ will have an impact on both, the central depression of an absorption line, and its wings. The higher $\log g$, the broader a line gets (Fig. 7.4). The change in central depression is a result of the increasing broadening caused by the effects discussed in chapter 5.

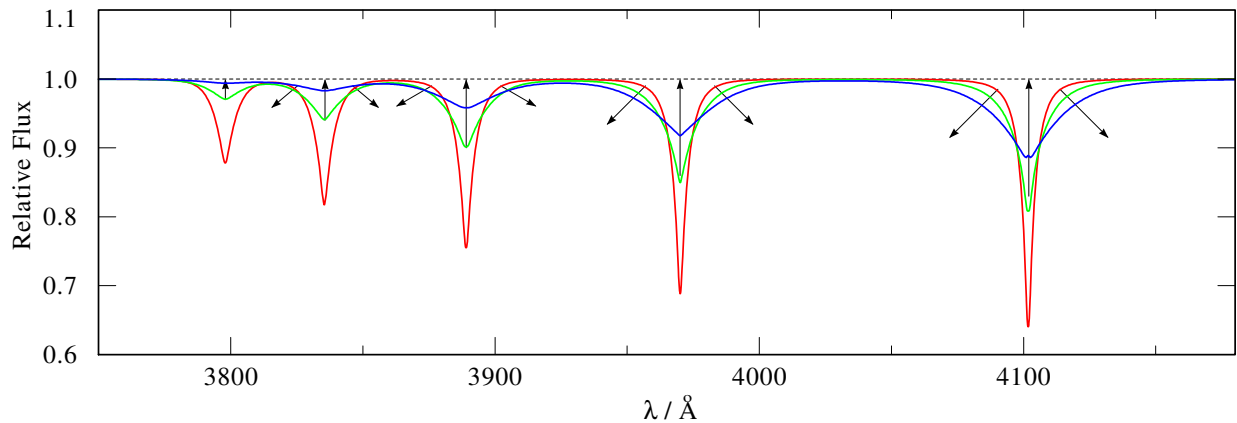


Figure 7.4: Lines at $\log g = 6$ (red), 7 (green), 8 (blue).

7.3 Element composition and mass ratio

A change in element composition results in a couple of fundamental changes in the corresponding spectrum. Here, mass ratios of the involved elements can be changed or extended for further elements. It is no surprise that new absorption lines will show and the existing lines of other elements will weaken, if the configuration of a model is extended by an additional element. If only the mass ratio of the existing elements is changed, the relative strength of absorption lines of different elements can be varied.

8 Approach of the parameter determination

TMAW does not fit the model spectra to the observation, but calculates them entirely independently and from scratch. This poses the necessity of a thorough comparison of the observation with the synthetic spectra in order to achieve precise results. If we start with an observation, the parameters of which are entirely unknown, it is useful to roughly narrow those down first. In the beginning, a basic grid for the parameters T_{eff} and $\log g$ can be requested. The increment of T_{eff} can be limited to about 20 000 K, so the first requests would be 40 000 K, 60 000 K, 80 000 K and 100 000 K. As the scale of $\log g$ is logarithmic, an increment of 1 can be chosen here, resulting in first models with $\log g = 5, 6, 7$.

Generally, it is not important to start with one particular parameter. It is nevertheless sensible to get an overview over $\log g$ first. If however, the analysis is started with T_{eff} , comparisons are most usually not very conclusive, as the absorption line wings will hardly fit the observation, which complicates the determination of the strength of the central depression.

Step 1a

In the beginning, the observation should be compared with a broad grid of models. The parameter T_{eff} stays unchanged at an arbitrary value in the middle temperature range. At the same time, the parameter $\log g$ is varied by values of 1. The resulting synthetic spectra are then plotted together with the observation. Looking at the most prominent absorption lines in order to evaluate the development of the single models is a favourable approach. From this first comparison a preliminary approximation for this parameter should be possible.

Step 2a

This preliminary result for $\log g$ can now be used for the first look at T_{eff} . The proceeding is the same. A couple of model spectra varied by 20000 K are examined together with the observation, in order to get an overview for T_{eff} . Usually, a good approximation can easily be determined.

Step 1b

Now step 1 is repeated. Again one parameter stays unchanged, while the other one is varied. As reasonable approximations have already been determined, those are used here. The determined temporary value for T_{eff} stays unchanged, while $\log g$ now varied more precisely (first decimal) around the temporary value determined earlier. The synthetic spectra are then plotted together

with the observation for comparison. Similar to step 1, the best fitting value for $\log g$ should be determined for the following second analysis regarding T_{eff} .

Step 2b

The $\log g$ value should be determined reasonably well now. As in step 2b, this value will now stay unchanged, while a more precise variation of T_{eff} is performed around the previously determined approximation. As usually, the results will be plotted and compared with the observation to find the model with the best agreement to the recorded spectrum.

Finishing step 2b, a good foundation for further detailed analyses has been set up by gradually narrowing down the possible parameters to make the model fit the observation to a great extent.

Steps 1 and 2 can be repeated in changing order as often as desired, depending on what the comparison with the observation suggests.

Generally, the analysis requires a great amount of sensibility for the continuous comparison of synthetic spectra with an observation.

Step 3

After good approximations for T_{eff} and $\log g$ could be found, it is possible to start looking at the element composition in the star's photosphere. The models used to determine the preliminary results for the first two parameters, should be processed with solar values for element composition, as it is a good starting point. On the TMAW interface, those are set by default.

Should models deviate significantly from the observation, a change of the element abundances should be considered. In such a case, special attention must be paid to absorption lines of different elements. Since the mass ratio between those is decisive, a look at the respective lines shows that they deviate to roughly the same extent from the observation with opposite tendencies.

Let's suppose that the mass ratio of the element abundances of H and He do not match the observed spectrum. From a comparison it could then become obvious that, for example, He lines are stronger than in the recorded spectrum, whereas H lines appear to be weaker. As a consequence, the next step would be to reduce the relative He abundance and increase the relative H abundance.

A repeated comparison with the observation and the examination of a couple of lines will be informative about the adequacy of the recent change.

A clear sign for the necessity of a significant change in the element composition is the existence

of lines in the synthetic spectra, that are not represented in the observation. Fig. 8.1 shows such a case. The lines for He I at 4025 Å and He II at 4026 Å and 4199 Å are clearly not represented in the observation. Naturally, if such lines show at places in synthetic spectra where they do not in the observation, the abundance of the respective element in the photosphere is much lower or non-existent.

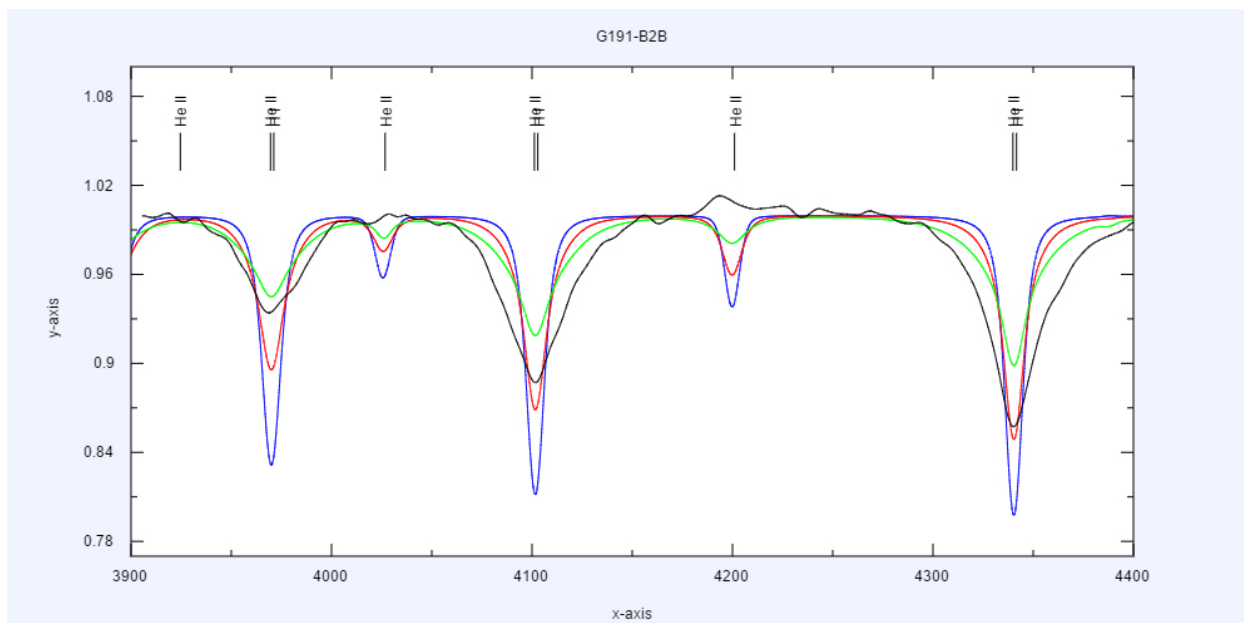


Figure 8.1: Observation of G191-B2B compared with three models at $T_{\text{eff}} = 60\,000\text{ K}$ and $\log g = 5$ (red), 6 (green), 7 (blue).

Source: <http://astro.uni-tuebingen.de/~TVIS/> 3.2.2017

The opposite case however, occurs on a regular basis. Strong absorption lines in an observation, which are not reproduced by synthetic spectra, are no exception. It can be explained by the constant development and improvement of atomic data. Most model atoms are so enormously elaborate and complex, that they cannot be included in model atmosphere calculations yet, as they are only slowly incorporated in the database over time.

A further possibility to adjust significant deviations of the synthetic spectra is the convolution of those with Gaussians. This changes the central depression and shape of the absorption lines in the synthetic spectra. Due to the limited resolving power of the used spectrographs, the recorded spectra do not fully represent the actual flux. This process is not taken into account in the calculations of synthetic spectra, but can be imitated by this process. An explanation of this effect can be found in chapter 10.4.

9 Examples

In this chapter two examples shall be examined and their parameters determined with the approach explained in chapter 8.

9.1 Example A

In this example the spectrum of the star Feige 66 shall be examined. The approach is similar to the steps mentioned in chapter 8. For the examination, the wavelength range from 3900 Å to 4500 Å will be analysed, because there are three prominent lines of the Balmer series, which offer a good opportunity for comparison. We start with a model that contains H and He with solar abundances.

Step 1a

First, we have a look at the wings of the absorption lines. In the beginning, T_{eff} will be kept at 80 000 K. Now $\log g$ can be plotted in three steps for comparison with the observation (fig. 9.1). The increment regarding $\log g = 1$.

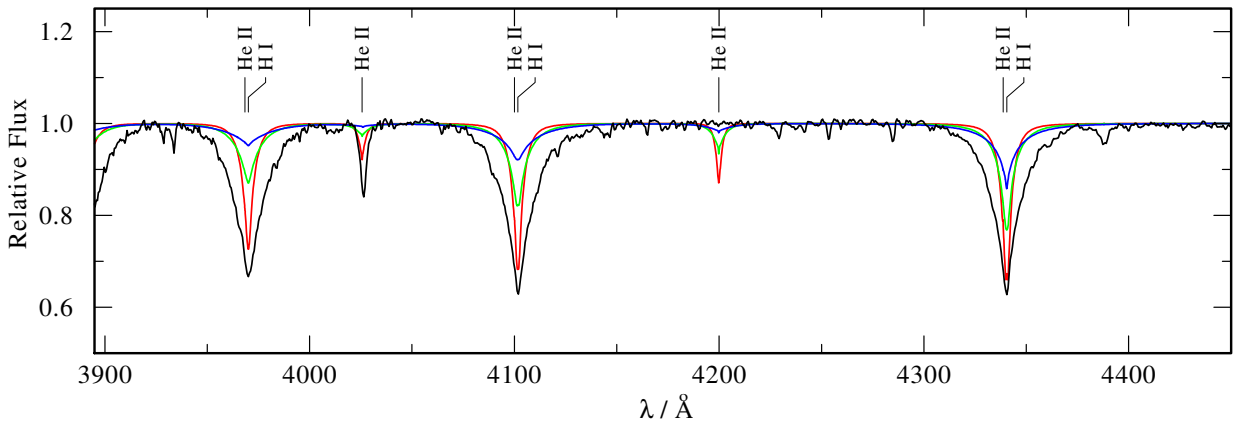


Figure 9.1: Observation of Feige 66 compared with three model spectra at $T_{\text{eff}} = 80\,000$ K and $\log g = 5$ (red), 6 (green), 7 (blue).

Looking at the line wings in direct comparison with the observation, the model with $\log g = 6$ reproduces the wings the best. Both other models are either too steep or too flat.

Step 2a

With the preliminary value of $\log g = 6$, we now turn to the first examination regarding T_{eff} . In this case, we try a grid with steps of 20 000 K.

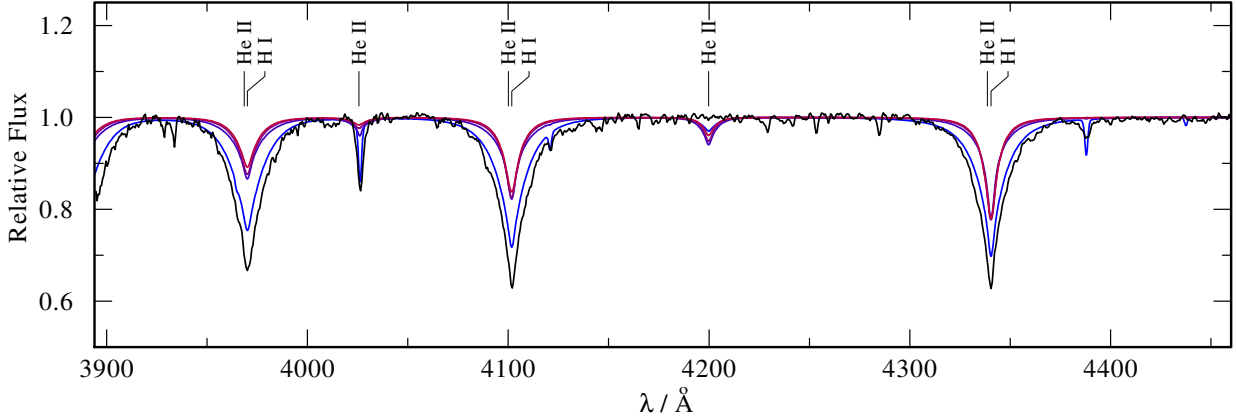


Figure 9.2: Observation of Feige 66 compared with four model spectra at $\log g = 6$. Steps from red to blue: $T_{\text{eff}} = 100\,000\text{ K}$, $80\,000\text{ K}$, $60\,000\text{ K}$, $40\,000\text{ K}$

It is clearly recognizable in fig. 9.2 that the approximation for $\log g$ is in the right scale. Furthermore, it is obvious that the models with $60\,000\text{ K}$, $80\,000\text{ K}$ and $100\,000\text{ K}$ significantly deviate from the observation. The model with $40\,000\text{ K}$ however, reproduces the it the best.

Step 2b

From step 2a it can easily be seen, that T_{eff} has to lie close to $40\,000\text{ K}$. In this case, it is sensible to consult a more precise grid, before moving on to $\log g$ again. As $40\,000\text{ K}$ still seems to hot, this should be the highest temperature of the new grid. In this more precise version, four models will be considered, with an increment of $5\,000\text{ K}$.

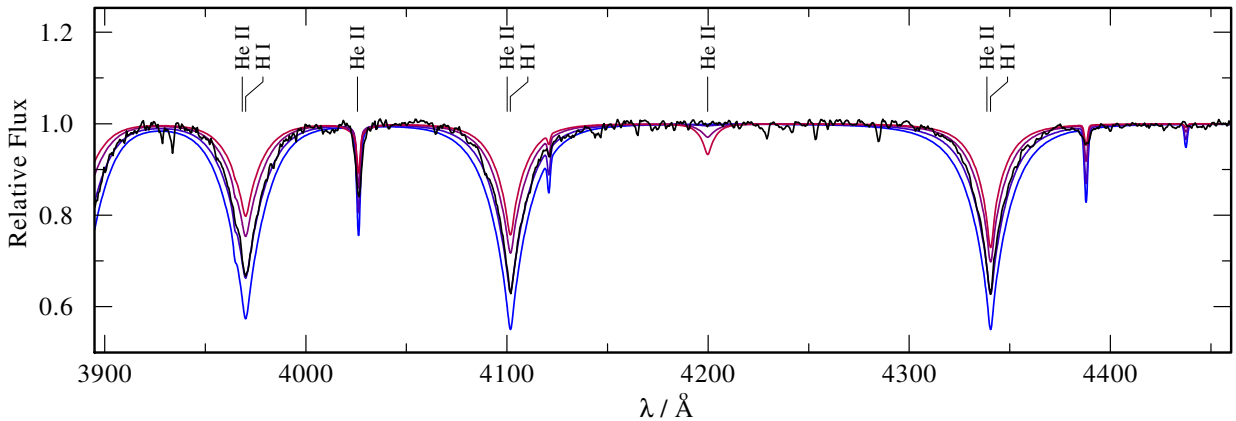


Figure 9.3: Observation of Feige 66 compared with four model spectra at $\log g = 6$. Steps from red to blue: $T_{\text{eff}} = 45\,000\text{ K}$, $40\,000\text{ K}$, $35\,000\text{ K}$ $30\,000\text{ K}$.

In this case (fig. 9.3), the model with $T_{\text{eff}} = 35\,000\text{ K}$ lies directly on the observation. The He II line

at about 4200 Å vanishes at this temperature.

Step 1b

T_{eff} has been narrowed down precisely in step 2b. A final consideration of $\log g$ will have to proof, whether the chosen surface gravity is correct. Thus, three models of an 0.2 increment around the temporary value from step 1a are plotted together with the observation.

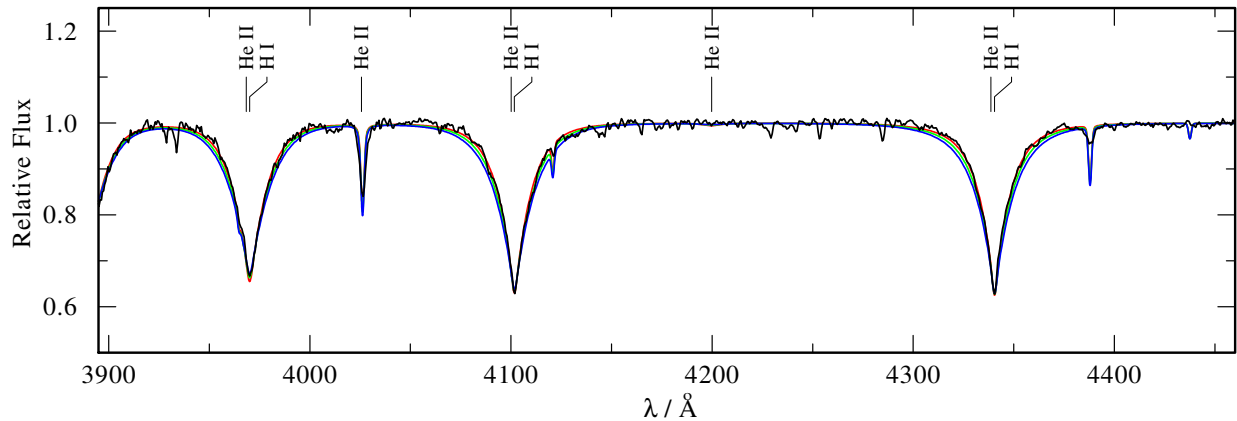


Figure 9.4: Observation of Feige 66 compared with three model spectra at $T_{\text{eff}} = 35\,000\text{ K}$ and $\log g = 5.8$ (red), 6.0 (green), 6.2 (blue).

The comparison in fig. 9.4 suggests, that a model with $\log g = 5.8$ lies closest to the recorded spectrum.

Step 3

There are no lines in the model that are not matched by the observation. Additionally, all lines in the observation are reproduced correctly. An adjustment of element abundances is not necessary.

Literature values

The values for this object found in literature are (1):

$$T_{\text{eff}} = 36.000 \pm 1000\text{ K}$$

$$\log g = 6 \pm 0.2$$

The applied method achieves results very close to the literature values in few uncomplicated steps.

9.2 Example B

In this example a spectrum of the star G191-B2B will be examined. Again, we will look at the wavelength range of 3900 Å to 4400 Å, as it includes very prominent Balmer lines. As in example A, we will start with models with solar abundances of the elements H and He.

Step 1a

As previously, T_{eff} is kept unchanged, this time at 60 000 K. At the same time $\log g$ is varied between 5 and 7 with an increment of 1.

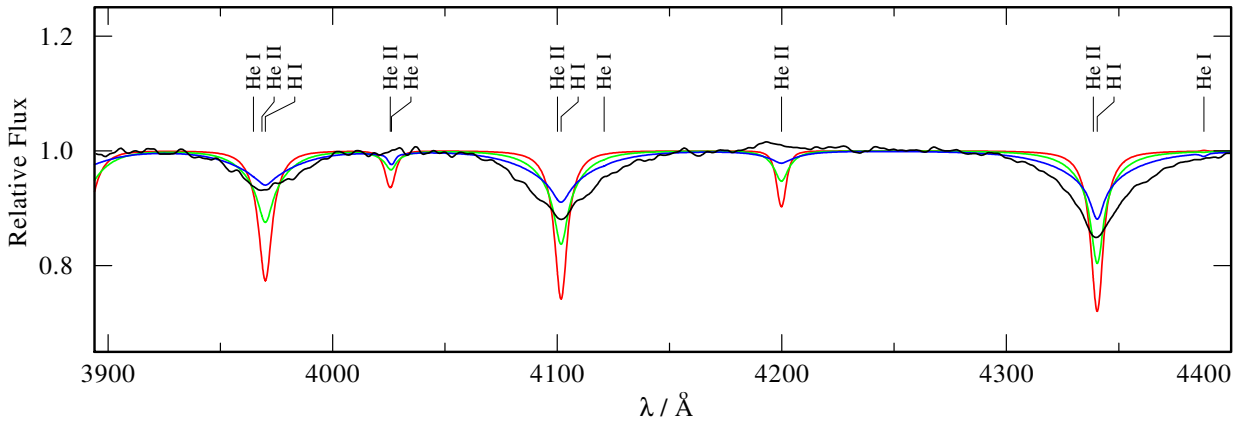


Figure 9.5: Observation of G191-B2B compared with three model spectra at $T_{\text{eff}} = 60\,000$ K and $\log g = 5$ (red), 6 (green), 7 (blue).

Fig. 9.5 shows, that $\log g = 7$ reproduces the observation best. However, it is clear that the models produce strong He lines (He I at 4025 Å and He II at 4026 Å and 4199 Å), which can not be found in the observation. Therefore step 3 is given priority.

Step 3

Since these lines can be attributed to helium, it is necessary to exclude this element from the models and continue the analysis with a pure H model.

Step 2a

After step 1a, models with $\log g = 7$ will be examined with a 20 000 K temperature increment.

In fig. 9.6 the decision is not easy. The central depression seems to increase quicker from line to line than in the observation. Consequently, the models do not yet fit the observation. Nevertheless the model with 80 000 K can be determined as the one matching the observation best. The rest of the analysis will be done with this value.

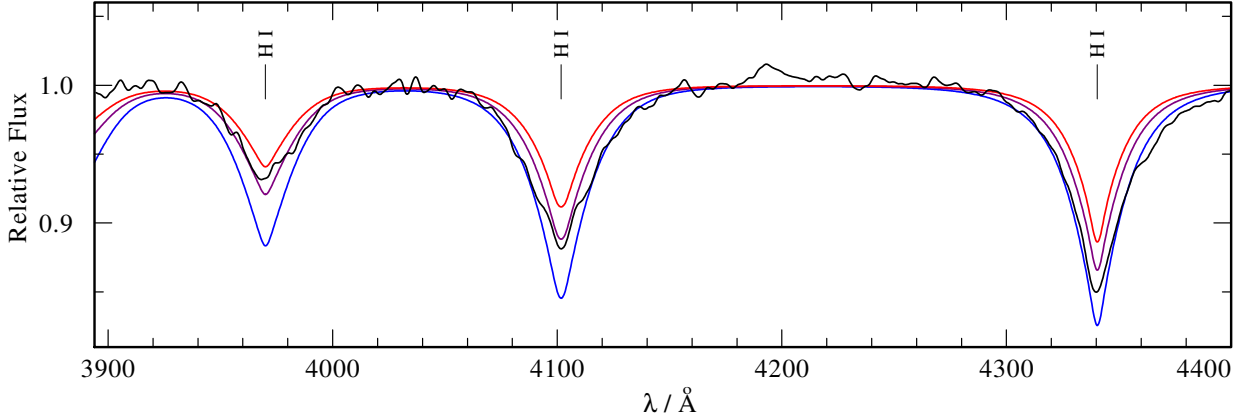


Figure 9.6: Observation of G191-B2B compared with three model spectra at $\log g = 7$. Steps from red to blue: $T_{\text{eff}} = 100\,000\text{ K}$, $80\,000\text{ K}$, $60\,000\text{ K}$.

Step 1b

Now the observation is compared with models of a more precise variation in $\log g$, since the models still show clear deviations from the recorded spectrum. A increment of $\log g = 0.5$ is sensible.

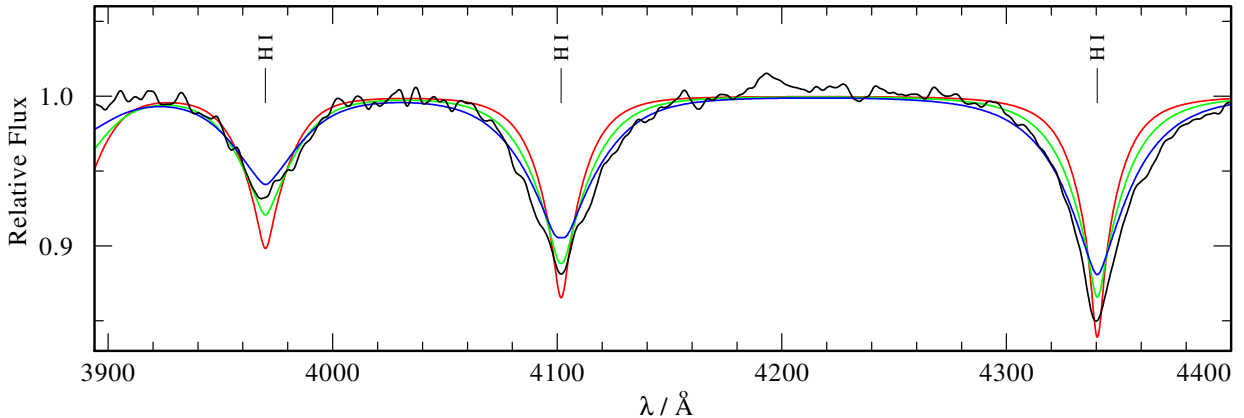


Figure 9.7: Observation of G191-B2B compared with three model spectra at $T_{\text{eff}} = 80\,000\text{ K}$ and $\log g = 6.5$ (red), 7.0 (green), 7.5 (blue).

Also in fig. 9.7 it is difficult to determine the best model. Especially at the absorption line at 3790 \AA , it is difficult to find the right model. However, looking at the line wings at the absorption lines at 4101 \AA and 4340 \AA , the model with $\log g = 7.5$ matches the observation better than the other models. The central depression does not seem to be right yet, which necessitates step 2b.

Step 2b

Fig. 9.7 illustrates that the central depression of the lines needs to be stronger. We could simply try another precise variation of T_{eff} around the current value, but from fig. 9.6 it is clear that the

stronger lines can be attributed to lower T_{eff} . This is why it is useful to use this value as the highest temperature for this comparison. Therefore a plot with models of T_{eff} 75 000 K, 70 000 K and 65 000 K, should allow better conclusions regarding this parameter.

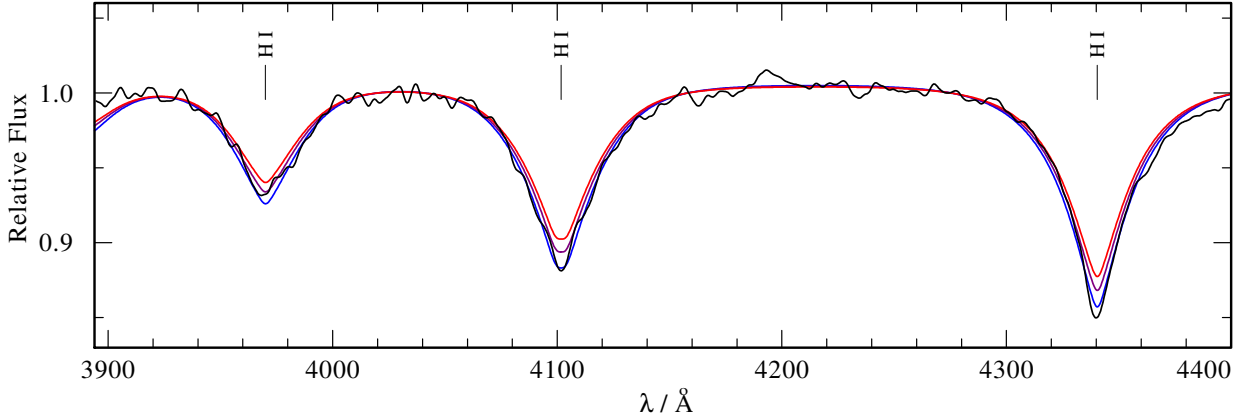


Figure 9.8: Observation of G191-B2B compared with three model spectra at $\log g = 7.5$. Steps from red to blue: $T_{\text{eff}} = 75\,000\text{ K}$, $70\,000\text{ K}$, $65\,000\text{ K}$.

The more precise the parameter grid, the more difficult it gets to determine the model matching the observation best. Fig. 9.8 requires a second gaze in order to recognize that the model with 65 000 K is the best. Since the line wings still do not match the observation, a last examination of $\log g$ will be made.

Step 1c

The 65 000 K from the last step will remain unchanged here again and $\log g$ is again varied more precisely with an increment of 0.1.

It is difficult to determine which model matches the observation best in fig. 9.9. It is clear that the model with $\log g = 7.5$ is the worst. Also, the model with $\log g = 7.7$ deviates a bit more from the observation at the outer lines. Therefore, the model with $\log g = 7.6$ reproduces the observation the best. As the comparison is done by eye, there will always be a certain amount of subjectivity involved and the values determined at very small differences in parameters can sometimes vary from the actual values.

Literature values

The values for this object found in literature are (2):

$$T_{\text{eff}} = 60\,000 \pm 2000\text{ K}$$

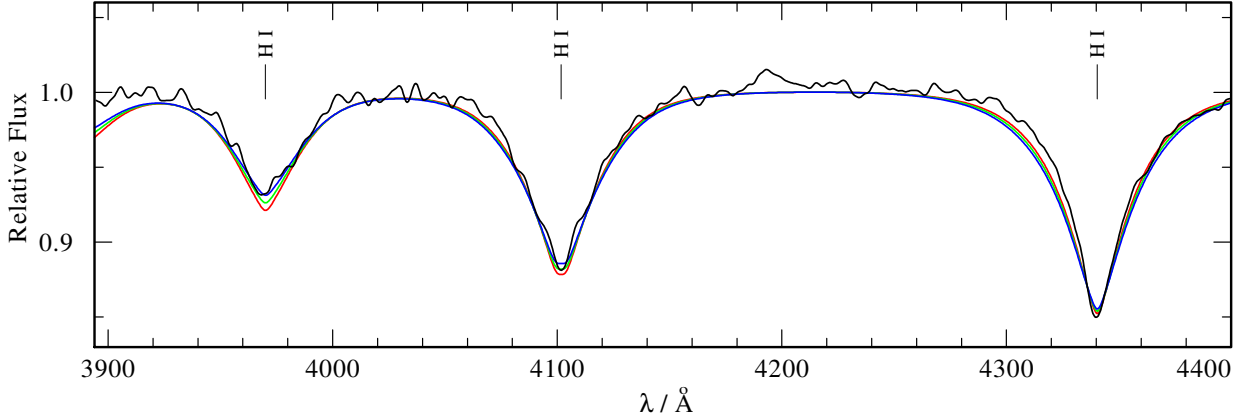


Figure 9.9: Observation of G191-B2B compared with three model spectra at $T_{\text{eff}} = 65\,000\text{ K}$ and $\log g = 7.5$ (red), 7.6 (green), 7.7 (blue).

$$\log g = 7.6 \pm 0.05$$

In this case, the used approach also reaches values close to those determined by precise and laborious scientific analyses.

Fig. 9.10 schematically illustrates the approach for the determination of parameters of an observation. First, a broad grid of parameters is created. This is then narrowed down step by step. The red arrows indicate the single parts of the examination from example 2. The scheme has the dimensions T_{eff} and $\log g$, consequently, a change in direction indicates the alternating examination of the two parameters.

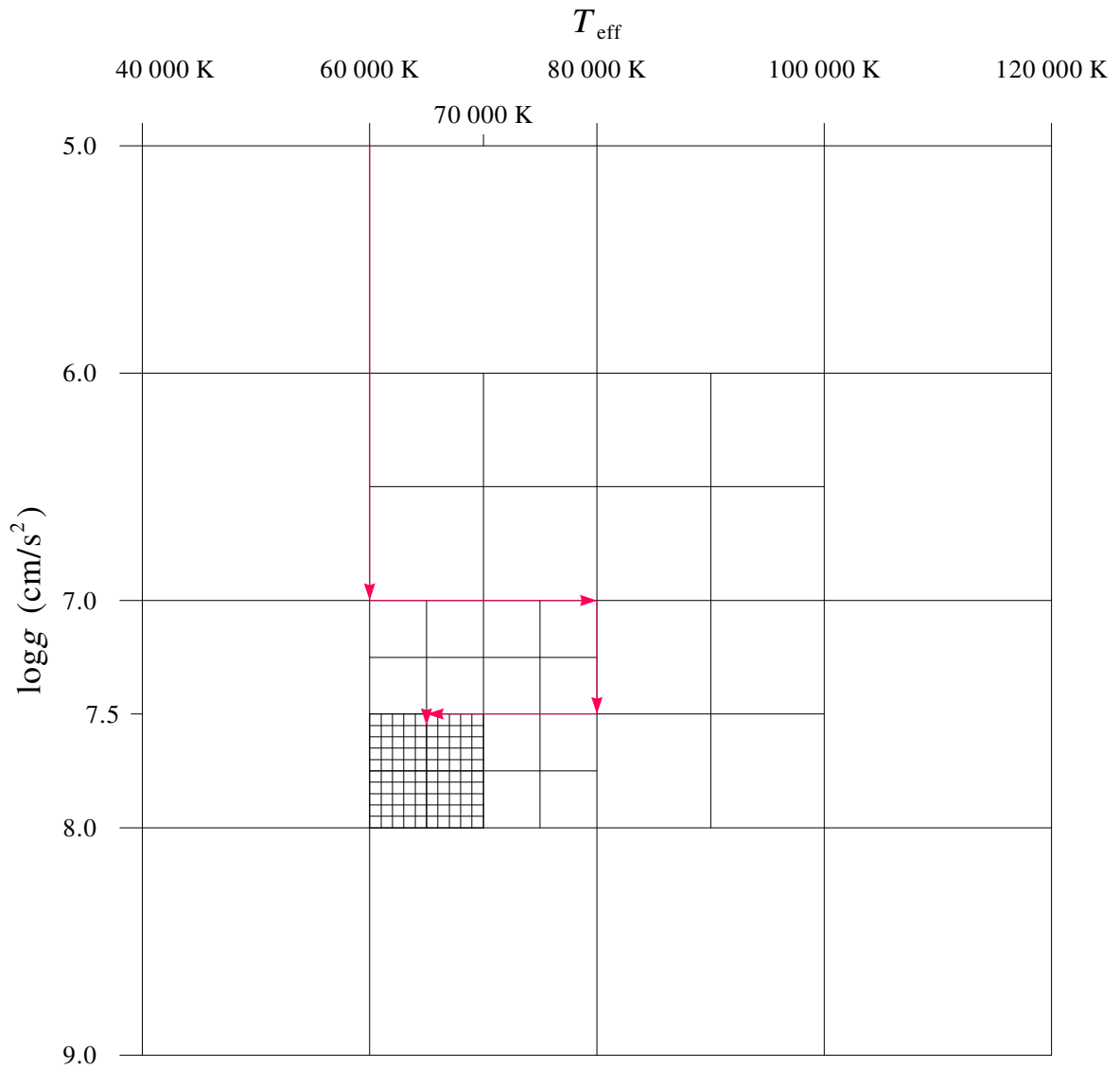


Figure 9.10: The approach for the parameter determination in a schematical representation.

10 Spectral analysis on the internet

The Institute for Astronomy and Astrophysics of the University of Tübingen is always eager to render its work tangible and accessible for the public. Everyone shall be able to participate in, and profit from our research. For this reason, several programs and a database have been launched online in the recent past. For both professional and amateurs alike, they offer the opportunity to carry out analyses online. In the course of this thesis, the following tools shall be explained:

TheoSSA: Theoretical Stellar Spectra Access is a database in which all synthetic spectra are accessible, which have been calculated in the past, for example by **TMAW**.

TMAW: Tübingen Model-Atmosphere Package WWW interface, the calculation of synthetic spectra, which do not yet exist in **TheoSSA**, can be commissioned.

TVIS: Tübingen Visualisation tool enables users to permanently embed a plot of a spectral analysis on their homepage.

TVIS Interactive: The **Tübingen Visualisation tool Interactive** facilitates simple visual analyses of stellar spectra directly on the internet, with the help of synthetic spectra from **TMAW** and **TheoSSA**.

TVIS Data Changer: This tool converts (observation-)data, to make them compatible with the **TVIS** applications.

10.1 TheoSSA

This database is available at <http://dc.g-vo.org/theossa>. Fig. B.1 in the appendix shows the graphical user interface. In order to obtain the desired synthetic spectra, only a few specifications are necessary.

Effective temperature in K: A limitation of the temperature range can be specified here. If only one bound is specified, it serves as either lower or upper boundary for the request, depending on which field it is entered in.

Log g in cm/s^2 : Following same principle, the boundaries for $\log g$ can be entered here.

Mass loss rate in units of sun masses per year: The mass loss can be specified here. However, search requests are also successful without this specification. Currently, models of expanding star atmospheres are not available yet.

Mass ratio: With those fields, the chemical composition of a star can be specified. First, an element is chosen from the drop-down box. Then, its mass ratio is specified by a number between 0 and 1. Thus, 10% equals 0.1. As previously, it is also possible to only specify upper or lower boundaries.

Standard stars: Alternatively, specifications can also be chosen to be the same as those of the standard stars included in the drop down box.

Table: The sorting of the resulting table can be specified here. It can be sorted by elements, ascending **ASC** or descending **DESC**. Furthermore, the number of results can be limited as well.

Output format: This allows the user to specify the representation of the search results. Moreover, in the drop down box **More Output fields** additional information, to be displayed with the spectra, can be selected.

After the search request, the entered parameter are confirmed (fig B.3) and the results matching those are displayed in a table sorted by the previously specified preferences (fig B.2). If the cursor is moved across the column product key, thumbnail images of the respective spectra appear (fig. B.4). Apart from the parameters specified in the request, the table also shows the wavelength range, that is covered by each synthetic spectrum. When saving data, the column product key allows the user to choose from different data formats. In order to plot the data in **TVIS**, the data should be saved as *.txt* file. Should spectra be needed, that are not available through **TheoSSA**, they can be calculated with **TMAW**.

10.2 TMAW

This tool is available at <http://astro.uni-tuebingen.de/~TMAW>. Fig. B.5 shows the graphical user interface. **TMAW** allows the calculation of synthetic spectra with parameter configurations not available through **TheoSSA**. The model atmospheres are calculated by the Tübingen NLTE

Model-Atmosphere Package (TMAP (6)), which is used for research at our institute. A request is made with few specifications.

Personal information: Please make sure that the entered email address is correct. You will be asked to check it before your request is submitted.

SED parameter: The details **wavelength** and $\Delta\lambda$ (distance of data points) of the spectrum can be specified here. Individual or default settings can be chosen.

Model-Grid parameters: To ensure efficient examinations, **TMAW** does not calculate single models, but a model grid of different parameter configurations, analogous to the procedure mentioned in chapter 8 (fig. B.6). The grid has the dimensions T_{eff} and $\log g$. Upper and lower boundaries need to be specified. Additionally, the increment between models must be chosen. Both factors should be selected according to chapter 8, depending on the progress of the current examination.

Values for T_{eff} are limited to 20 000 K - 300 000 K. Values for $\log g$ are limited to 4.0 - 9.9.

Element abundances: Those are set to solar values by default, but can be changed individually.

The more elements are included in the model, the longer a calculation will take. If the elements up to O are included, calculations can take up to two days. These can turn into five days, if all elements up to Mg are included.

After a request was finalised by **submit**, a request confirmation with a summary of your personal as well as grid specific data shows (fig. B.7, B.8). The user is informed twice via email: As soon as calculations are started and when calculations are successfully finished. The synthetic spectra are attached to the second email via a link.

10.3 TVIS

This tool is available at <http://astro.uni-tuebingen.de/~TVIS>. Fig. B.11 shows the website. It contains step-by-step instructions on how to include the plotter on one's homepage, in order to present individual research on spectra to others. The tool is based on HTML5 and works without Java and Flash. Extensive layout options can be found under the link in the **Commands**-area

(fig. B.13), which allows the realisation of individual settings. Some examples can be found in the section **Objects**.

Furthermore, the TVIS Data Changer can be found on the **TVIS** (fig. B.14) page as well.

10.4 TVIS Data Changer

This tool optimises the files from **TMAW** and **TheoSSA**, which are ought to be plotted with **TVIS**. Redundant information is removed and the number of data points is reduced depending on the settings, in order to speed up the plotting process. The structure of **TMAW** or **TheoSSA** files is illustrated in chapter C.1. All lines starting with * are referred to as comment lines, which do not contain any usable information. They contain information on the developers of the process as well as the programmes involved in the calculation. Furthermore, the corresponding parameters are summed up. Thus, the * symbol represents the comment sign of the file in chapter C.1, which makes sure that everything contained in the respective lines is ignored as it is only meant to be a comment for the user.

The last six lines of the comment part specify what is contained in the following columns. Column one contains the wavelength, column two the absolute flux and column three the relative flux. For a smooth operation of the Data Changer, the most recent version of Java should be installed on the executing computer. Only a few specifications are necessary to obtain an improved data file:

Input: With the button **Browse**, the file can be selected from the directory of the user computer.

The file must have been saved from **TMAW** or **TheoSSA** previously. Furthermore, it is possible to optimise data recorded individually, all settings apply for those as well.

Output: With the button **Browse** the output folder and the name of the newly created file can be defined.

Comment sign: This field specifies which symbol acts as comment sign in the selected file, and which data can therefore be ignored. For files from **TMAW** or **TheoSSA** this will always be the * symbol, which is the default setting. For .txt files of other origin, the comment sign has to be checked in the file and entered here.

Define Column: Since the files from **TMAW** and **TheoSSA** may contain up to three columns,

the user has to specify which column ought to be plotted against which column. For examinations with rectified spectra, column one and three must be selected.

Re-grid: To reduce the amount of data further, the desired range of x values can be limited through **Xmin** and **Xmax**, which causes the data outside the entered limits to be ignored.

It is essential to make sure that the range from Xmin to Xmax does not exceed the available range given in the original file!

The value entered in **Grid** defines the distance between two data points (in integral numbers) on the x axis of the output file. The original values are interpolated accordingly. Chapter C.1 shows a file with **Xmin** = 915 and **Grid** = 2.

Convolve: When stellar spectra are recorded by a spectrograph, it never records the entire information. Due to their limited resolving power⁴, a recorded colour can only be attributed to either pixel A or pixel B right next to it. Within a pixel however, wavelengths can not be differentiated any further. Pixel A corresponds to a certain wavelength, and pixel B to a wavelength very close to the one from pixel A. Information is lost, because all the light reaching pixel A is only attributed to the respective wavelength, although a pixel still covers a small range of wavelengths.

The synthetic spectra from **TMAW** and **TheoSSA** do not take this effect into account, which is why it has to be added retrospectively through **Convolve** to allow good comparisons. Since the most spectrographs change the absorption line profiles towards a Gaussian, **Convolve Gauss** synthesises this effect and convolutes it with the synthetic spectra. This way, line profiles are changed to a realistic shape. **Box** represents the easiest smoothing function, whereas **Gauss** is more realistic. The magnitude of the effect is controlled by σ using **Gauss**, and by **Width** using **Box**. Normal values for σ lie between 0.01 (for high resolution spectra), 1 (for medium resolution) and up to 6 (for low resolution).

Calculate: Saves the optimised file in the selected directory. Chapter C.2 shows the modified file.

Unnecessary information was removed and the amount of data reduced according to the settings in **Grid**.

⁴ $r = \frac{\lambda}{\Delta\lambda}$

10.5 TVIS Interactive

This tool is available at <http://astro.uni-tuebingen.de/~TVIS/interactive>. Fig. 7.1 shows the graphic user interface. Unlike **TVIS**, the **TVIS Interactive** interface offers the opportunity to analyse recorded spectra directly on the internet by comparing them to synthetic spectra from **TMAW** and **TheoSSA**. The tool is designed to easily facilitate the approach illustrated in chapter 8 and 9. Up to three previously saved synthetic spectra can be plotted together with the observation.

Dataset 01 - 04: In these fields underneath the plot box, the synthetic spectra, observations and other files can be uploaded.

Identification: An additional line identification file can be uploaded here. There are, nevertheless, fundamental absorption lines of the elements **H** und **He** available as default identifications in the section **Default identification** on the right hand side.

Upload and Submit: After clicking this button, the files are uploaded and the plot is created. This may take some seconds.

Specifications can only be made after the spectra have been plotted already. Changes will then be realised instantaneously.

Header: The header for the plot can be specified in this field. The default setting is *Header*.

X_{min}/X_{max}: The x axis range of the plot data can be limited here (in Å).

Y_{min}/Y_{max}: Identically, the y axis range of the plot data can be limited here (in Å).

X_{Exp} or Y_{Exp} Notation: Activation of the box changes the axis labels to exponential notation. The fields **Digits** determine the number of decimals. The default setting is 2.

Datasets: In this section the colours of the plotted data sets can be selected from a drop down box. The field Y_{Ident} specifies the y position of the identification lines (in Å), should additional identification files be included. The default setting is Y_{min} . The colour can be changed as well.

Default identification: This section is concerned with the default line identifications. The elements **H** and **He** are covered. **Series** refers to the series illustrated in fig. A.2, which

have been extended by the first two ionisation stages of helium. The series can be added by activating the box.

Y_{Ident}: This specifies the position of the default identification lines. The default position is Y_{\min} , which is why it should be changed.

Crosshair: By activating this box, a horizontal and a vertical line are drawn through the top of the cursor. This can potentially simplify the determination of the exact positions of central depressions or peaks in the spectrum.

Save Plot: The displayed plot can be saved in PNG-format for further usage. Unfortunately, this function only works in Firefox, but not in the Microsoft Internet Explorer, at the time this thesis was completed.

Test spectra: In order to familiarise yourself with the approach explained in chapter 8 and 9 without having to provide own spectra, this section contains several real and synthetic spectra and the respective literature values. Those can be downloaded for testing **TVIS Interactive**.

11 Spectrometers in school

In the course of this thesis, spectrometers commonly used school have been tested for their suitability to examine stellar absorption line spectra. The two most common models were analysed:

- 1.) The SPECTRA - 1 of the company Kvant Ltd. (fig. 11.1 a).
- 2.) The SPECTRA mini from Cornelsen Experimenta (fig. 11.1 b).



(a) The SPECTRA - 1 from Kvant Ltd.

(b) The SPECTRA *mini* from Kvant Ltd.

Figure 11.1: Spectrometer commonly used in school.

After both models were delivered, it soon turned out that, although the SPECTRA mini had been distributed by Cornelsen Experimenta, it was in fact a product of Kvant. While the SPECTRA mini is a bit smaller than the SPECTRA - 1, the included software SPECTRA₁ is identical. The interface is shown in fig. B.16. Already after the first launch of the software it turned out that the analysis of stellar spectra would be impossible.

The user interface is easy to use and very intuitively. The representation of spectra is realised very well for the use in schools. A real, coloured image of the recorded spectrum is shown, and the corresponding spectral energy distribution can be coloured depending on the depicted wavelengths. A very useful serial image function is included, which allows to capture good spectra during a short influx of light (e.g. deflagrations). Moreover, multiple spectra can be plottet simultaneously for comparison.

Despite the advantageous setup of control features for the use in schools, the program does not allow to control the exposure time, which is of essential importance when recording stellar spectra

with low luminosity. Furthermore, the unit of flux is neither provided in the graph nor in the data which can be exported. However, decisive for the suitability of the spectrometer for the examination of stellar spectra is its resolution. Looking at an output file, which is identical for both models, it becomes clear that the resolution is not sufficient enough. A resolving power of 4-5 Å does unfortunately not meet the requirements necessary for the examination of normal spectra.

The model SPECTRA - 1 has been provided by **Kvant Ltd.**⁵ with friendly assistance.

The model SPECTRA mini has been provided by **Cornelsen Experimenta**⁶ with friendly assistance.

⁵<http://www.kvant.sk/en/home>

⁶<http://www.corex.de>

References

- [1] B. Baschek, P. Hoefflich, and M. Scholz. The OB subdwarf Feige 66, a chemical-composition twin to HD 149382. *A&A*, 112:76–83, August 1982.
- [2] B. Baschek, P. Hoefflich, and M. Scholz. The OB subdwarf Feige 66, a chemical-composition twin to HD 149382. *A&A*, 112:76–83, August 1982.
- [3] The Star Garden. Newtons theory of light. <http://www.thestargarden.co.uk/Newtons-theory-of-light.html>, Dec 2016.
- [4] P.A. Tipler and G. Mosca. *Physik für Wissenschaftler und Ingenieure*. Spektrum Akademischer Verlag, Heidelberg, 6. edition, 2009.
- [5] A. Weigert, H.J. Wendker, and L. Wisotzki. *Astronomie und Astrophysik: ein Grundkurs*. Wiley-VCH, Weinheim, 5., aktualisierte und erw. aufl., 2. nachdr. edition, 2011.
- [6] K. Werner, S. Dreizler, and T. Rauch. TMAP: Tübingen NLTE Model-Atmosphere Package. Astrophysics Source Code Library [record ascl:1212.015], December 2012.

A Absorption lines quantitative

Bohr's idea of discrete circular orbits was motivated by the fact, that accelerated charge in magnetic fields emits radiation, which would eventually cause such an energy loss that the electrons would fall into the atoms core. To avoid this, Bohr postulated in three postulates (4) that electrons could move lossless, without emitting electromagnetic radiation, on those orbits.

1st postulate

Orbits in an atom, and thus energy levels, only exist stationary with steps of E_n .

2nd postulate

The frequency of the emitted electromagnetic radiation is equal to the energy difference between the corresponding energy levels, following

$$h\nu = E_B - E_A \quad . \quad (14)$$

3rd postulate

The revolution of electrons is only possible on special orbits. This is described by a quantised angular momentum, which can only occur as an even multiple of \hbar (Planck's constant, $\hbar=6.62610^{-34}\text{Js}$), expressed as

$$L = mv_n r_n = \frac{n\hbar}{2\pi} = n\hbar, n \in \mathbb{N} \quad . \quad (15)$$

n is the principal quantum number. Naturally, the Coulomb force F_c acts as centripetal force F_z to the inside on those circular orbits, which can be expressed as

$$F_z = F_c \quad (16)$$

$$\frac{1}{4\pi\epsilon_0} \frac{Ze^2}{r^2} = \frac{m_e v^2}{r} \quad . \quad (17)$$

Eq. 17 rearranged for v results in

$$v^2 = \frac{Ze^2}{4\pi\epsilon_0 m_e r} \quad . \quad (18)$$

Here ϵ_0 is the dielectric constant, m_e the mass of the electron, Z the atomic number and r the orbit radius.

This determines the velocity parameter, since all parameters are set for the corresponding elements. Now the third postulate can be used as a condition for the velocity (Eq. 19). It expresses that the angular momentum can no longer be any value, but has to be an even multiple of \hbar , which is why it is called quantised angular momentum .

$$L = m_e v_n r_n = \frac{n\hbar}{2\pi} = n\hbar, n \in \mathbb{N} \quad (19)$$

$$m_e v_n r_n = n\hbar \quad (20)$$

Eq. 20 again rearranged for v results in

$$v_n = \left(\frac{n\hbar}{m_e r_n} \right)^2 \quad . \quad (21)$$

This inserted in Eq. 18 results in

$$\frac{Ze^2}{4\pi\epsilon_0 m_e r} = \left(\frac{n\hbar}{m_e r_n} \right)^2 \quad | : r \quad (22)$$

$$\frac{Ze^2}{4\pi\epsilon_0 m_e} = \frac{n^2 \hbar^2}{m_e^2 r_n} \quad . \quad (23)$$

Eq. 23 can now be rearranged for r which results in

$$r_n = 4\pi\epsilon_0 \frac{n^2 \hbar^2}{Ze^2 m_e} = \frac{4\pi\epsilon_0 \hbar^2 n^2}{e^2 m_e Z} \quad . \quad (24)$$

After inserting the third postulate as side condition, it is clear that only certain orbits with a set radius can exist, depending on the principal quantum number n . This discrete distribution of possible orbits also has an effect on the total energy of the orbiting electrons. The potential energy

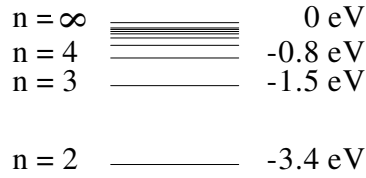
of an electron on an orbit in an electromagnetic field is described by

$$E_{\text{pot}} = -\frac{1}{2} \frac{1}{4\pi\epsilon_0} \frac{Ze^2}{r} \quad . \quad (25)$$

With the possible orbits r_n calculated above, the resulting energy levels for an atom with atomic number Z are

$$E_n = -\frac{1}{2} \left(\frac{1}{4\pi\epsilon_0} \right)^2 \frac{Z^2 e^4 m_e}{\hbar^2 n^2} = -Z^2 \left[\frac{e^4 m_e}{(4\pi\epsilon_0)^2 \hbar^2} \right] \frac{1}{n^2} = Z^2 E_0 \frac{1}{n^2} \quad . \quad (26)$$

Here, E_0 describes the binding energy in the ground state. This equation allows us to determine the different energy levels of an atom. Fig. A.1 shows the first levels of hydrogen ($Z=1$) starting from the ground state with $n=1$. In this case the ground state is $E_0 = -13.6$ eV.



$n = 1$ ===== -13.6 eV

Figure A.1: Energy levels of hydrogen.

In order to move an electron from energy level A to energy level B, the required and clearly defined amount of energy is

$$E_{\text{AB}} = Z^2 E_0 \frac{1}{n_B^2} - Z^2 E_0 \frac{1}{n_A^2} = -Z^2 E_0 \left(\frac{1}{n_B^2} - \frac{1}{n_A^2} \right) \quad . \quad (27)$$

This equation is known as Rydberg formula. It allows us to expand the level scheme for transitions

between orbits of higher principal quantum numbers.

Different transitions starting from the same energy level can be put together in series, as illustrated in fig A.2. Concerning hydrogen, the series that is made up by transitions from the first level is called Lyman series, for transitions from the second level the series is called Balmer series.

However, in reality this transition scheme gets a lot more complicated, the more electrons an element has. In multi-electron systems, a great variety of electron configurations can be realized and with it even more transitions. Every single ionisation stage of an element extends the number of transition possibilities significantly.

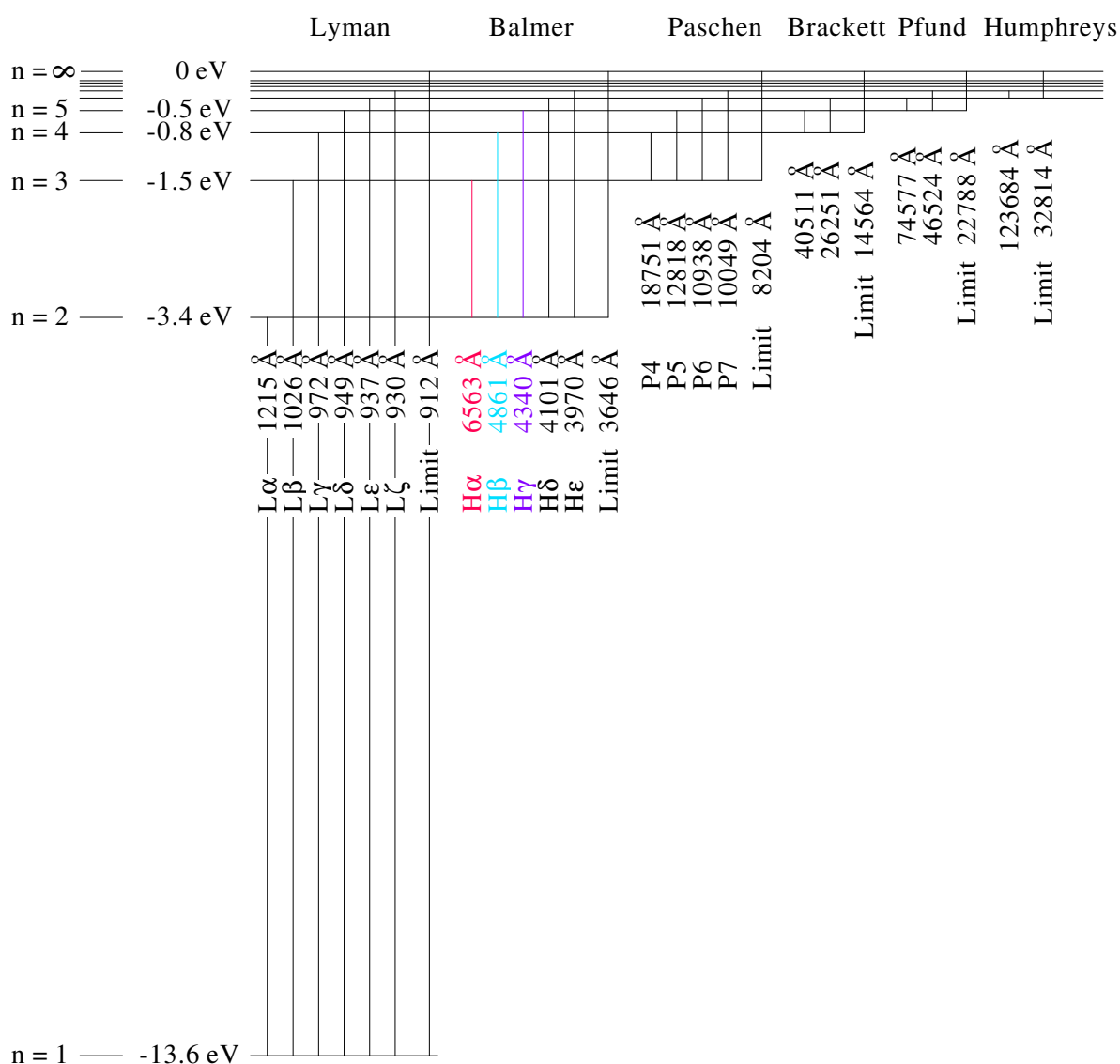


Figure A.2: Transition series in hydrogen.

Within a particular atom configuration, those transitions are usually visualised by Grotrian diagrams, which illustrate the complexity of the processes. As an example, fig. A.3 shows the Grotrian diagram of neutral helium. In the quantum-mechanical approach to this configuration, there are four equally valid solutions to the Schrödinger equation. Those only differ in their spin functions (which determine the spin configuration of the involved electrons). Three of those four solutions reproduce identical energy levels and one produces energy levels different to those. The result are two equally valid transition schemes, which depend on different spin configurations. On the left hand side, the singlet solution is shown. Its energy levels are only produced by one electron spin configuration. On the right hand side, the triplet solution is illustrated, where the energy levels are produced identically by three different electron spin configurations. All those possible configurations, transitions and their probabilities, as well as population density of the excited states are included in the calculations of model atmospheres in dependence of the respective parameters. This explains why calculations can take up to days, even on high-performance computers.

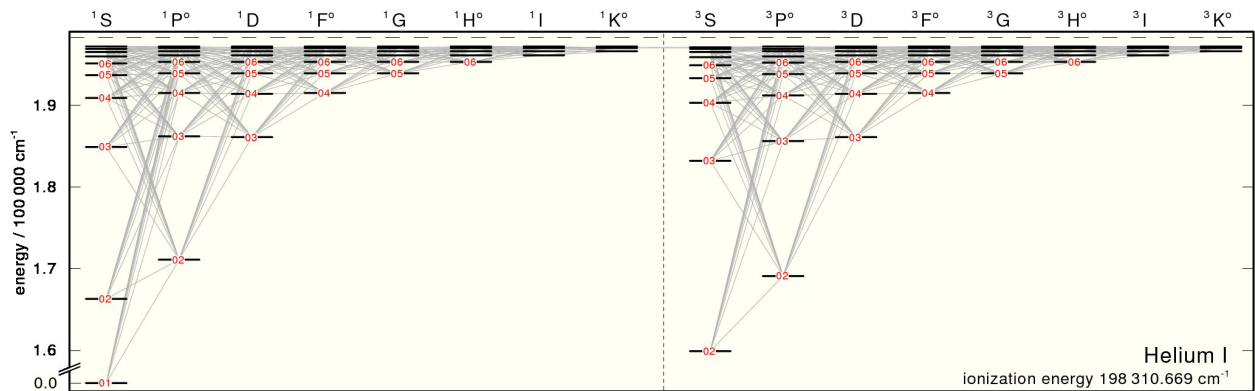


Figure A.3: Grotrian diagram of neutral helium.
 Source: <http://astro.uni-tuebingen.de/~TMAD>, 14.12.2017.

In order to perform a transition to a higher level, an influx of energy is required. The amount of energy that is necessary, can be supplied through different ways. The required energy can be transferred through a collision of atoms with ions, electrons or other atoms. Nevertheless, the transition induced by the absorption of light is of special interest for us. If the kinetic energy of a photon equals the amount energy that is required to perform a level transition, the atom can absorb the photon and will be transferred into an excited state. Following Planck, the energy of a photon

is closely related with its wavelength λ and, thus, with its colour.

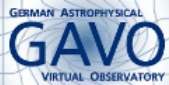
$$E = h\nu = \frac{hc}{\lambda}; \quad \lambda = \frac{hc}{E} \quad (28)$$

Thereby the wavelength is linked with the energy through the Rydberg formula

$$\Delta E = Z^2 E_0 \left(\frac{1}{n_B^2} - \frac{1}{n_A^2} \right) \quad . \quad (29)$$

Therefore, every transition in an element absorbs light of a particular wavelength.

B Homepages



Help

Service info

Related

[Compute custom SEDs](#)

Metadata

Identifier
ivo://org.gavo.dc/theossa/c

Cite this
[Advice on citing this resource](#)

Description
TheoSSA provides spectra

Keywords
Stars: atmospheres

Creator
Rauch, T.

Created
2010-11-11T15:00:00

Data updated
2016-11-28

Copyright
When publishing research please acknowledge: "The

Source
[2003ASPC...288..103R](#)

Reference URL
[Service info](#)

TheoSSA TMAP Web Interface

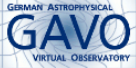
TheoSSA provides spectral energy distributions based on model atmosphere calculations. Currently, we serve results obtained using the Tübingen NLTE Model Atmosphere Package (TMAP) for hot compact stars.

Effective Temperature [K]	between	<input type="text"/>	and	<input type="text"/>	<small>Range of the atmosphere's effective temperatures to include. If you only specify one bound, you get a half-infinite interval.</small>
Log. Surface gravity [cm/s ²]	between	<input type="text"/>	and	<input type="text"/>	<small>Range of surface gravities to include. If you only specify one bound, you get a half-infinite interval.</small>
Mass loss rate [solMass/yr]	between	<input type="text"/>	and	<input type="text"/>	<small>Range of mass loss rates to include. If you only specify one bound, you get a half-infinite interval.</small>
Mass Fraction 1	<input type="text" value="ANY"/> between	<input type="text"/>	and	<input type="text"/>	<small>Mass fraction of an element. You may leave out either upper or lower bound.</small>
Mass Fraction 2	<input type="text" value="ANY"/> between	<input type="text"/>	and	<input type="text"/>	<small>Mass fraction of an element. You may leave out either upper or lower bound.</small>
Mass Fraction 3	<input type="text" value="ANY"/> between	<input type="text"/>	and	<input type="text"/>	<small>Mass fraction of an element. You may leave out either upper or lower bound.</small>
Standard Stars	<input type="text" value="EG 274"/> <input type="text" value="Feige 67"/> <input type="text" value="Feige 110"/>	<small>No selection matches all, multiple values legal. Common name of object observed.</small>			
Table	Sort by	<input type="text"/>	ASC	<input type="text"/>	
	Limit to	<input type="text" value="100"/>	items.		
Output format	<input type="text" value="HTML"/>	<input type="button" value="More output fields"/>			

When publishing research making use of this service, please acknowledge: "The TheoSSA service (<http://dc.g-vo.org/theossa>) used to retrieve theoretical spectra for this paper was constructed as part of the activities of the German Astrophysical Virtual Observatory."

Figure B.1: The TheoSSA homepage.

Source: <http://dc.g-vo.org/theossa>, 12.01.2017



GERMAN ASTROPHYSICAL
GAVO
VIRTUAL OBSERVATORY

Help

Service info

Related

[Compute custom SEDs](#)

Metadata

Identifier
ivo://org.gavo.dc/theossa/c

Cite this
[Advice on citing this resource](#)

Description
TheoSSA provides spectra

Keywords
Stars: atmospheres

Creator
Rauch, T.

Created
2010-11-11T15:00:00

Data updated
2016-11-28

Copyright
When publishing research
cite the following information:
The

Source
[2003ASPC...288..103R](#)

Reference URL
[Service info](#)

[Try ADQL to query our data.](#)

Please report errors and problems to the [site operators](#).
Thanks.
[Privacy](#) | [Disclaimer](#)
[Log in](#)

TheoSSA TMAP Web Interface

Parameters

- Element 1: H
- Max Effective Temperature [K]: 80000
- Max Log. Surface gravity [cm/s²]: 5.8
- Max. Mass Fraction 1: 0.9
- Min Effective Temperature [K]: 60000
- Min Log. Surface gravity [cm/s²]: 5.2
- Min. Mass Fraction 1: 0.7

Result

Matched: 36

[Send via SAMP](#) [Quick Plot](#)

Collection	Product key	Band start [Angstrom]	Band end [Angstrom]	Eff. Temp. [K]	Log Grav. [cm/s ^{**2}]	Mass loss rate [solMass/yr]	H	He	C	N	O	F	Na
	[...as VOTable] [...as Text] [...in Specview]	5.00	2000.00	60000	5.5	0.0	0.8	0.2	0.0	0.0	0.0	0.0	0.0
	[...as VOTable] [...as Text] [...in Specview]	2000.00	3000.00	60000	5.5	0.0	0.8	0.2	0.0	0.0	0.0	0.0	0.0
	[...as VOTable] [...as Text] [...in Specview]	3000.00	55000.00	60000	5.5	0.0	0.8	0.2	0.0	0.0	0.0	0.0	0.0
	[...as VOTable] [...as Text] [...in Specview]	5.00	2000.00	60000	5.5	0.0	0.9	0.1	0.0	0.0	0.0	0.0	0.0
	[...as VOTable] [...as Text] [...in Specview]	2000.00	3000.00	60000	5.5	0.0	0.9	0.1	0.0	0.0	0.0	0.0	0.0
	[...as VOTable] [...as Text] [...in Specview]	3000.00	55000.00	60000	5.5	0.0	0.9	0.1	0.0	0.0	0.0	0.0	0.0

Figure B.2: Output table of TheoSSA.
Source: <http://dc.g-vo.org/theossa>, 12.01.2017

Parameters

- Element 1: H
- Max Effective Temperature [K]: 80000
- Max Log. Surface gravity [cm/s²]: 5.8
- Max. Mass Fraction 1: 0.9
- Min Effective Temperature [K]: 60000
- Min Log. Surface gravity [cm/s²]: 5.2
- Min. Mass Fraction 1: 0.7

Figure B.3: Confirmation of the parameters.
Source: <http://dc.g-vo.org/theossa>, 12.01.2017

Collection	Product key	Band start [Angstrom]	Band end [Angstrom]	Eff. Temp. [K]	Log Grav. [cm/s**2]
	[...as VOTable] [...as Text] [...in Specview]	5.00	2000.00	60000	5.5
	[...as VOTable] [...as Text] [...in Specview]	2000.00	3000.00	60000	5.5

Figure B.4: Preview of the synthetic spectra.
Source: <http://dc.g-vo.org/theossa>, 12.01.2017

[Home](#)

[About GAVO](#)

[Getting Started](#)

[GAVO Data Center](#)

[Documents](#)

[Internal](#)

Search

[Login](#)

Sponsored by



Member of the International
Virtual Observatory Alliance



TMAW Request

Please specify effective temperature T_{eff} , surface gravity $\log g$, abundances for H, He, C, N, O, Ne, Na, and Mg as well as your e-mail address.

A NLTE model atmosphere with your input parameters will be calculated by *TMAP* - the Tübingen NLTE Model-Atmosphere Package - and you will be informed about the progress by e-mail.

Personal Information

Last Name
 First Name
 Institute
 E-mail

SED Parameters

Wavelength range for standard SED:
 5 - 2000 Å 2000 - 3000 Å 3000 - 55000 Å

Wavelength range for an individual SED and a quicklook plot:

3500 - 7000 Å, $\Delta\lambda \approx$ 0.1 Å

Note: the maximum number of data points is about 50 000.

Before submitting, please verify the data you entered, especially your e-mail address.

When publishing research making use of this tool, please acknowledge:
 "The TMAW tool (<http://astro.uni-tuebingen.de/~TMAW>) used for this paper was constructed as part of the activities of the German Astrophysical Virtual Observatory."

WEB : This page was visited **2 7 4 1** times since June 2, 2008

Model-Grid Parameters

T_{eff} [K]: 20 kK $\leq T_{\text{eff}} \leq$ 300 kK
 T_{eff} [K] (pure H+He): 20 kK $\leq T_{\text{eff}} \leq$ 1 MK
 Minimum 100000 Maximum 20000 Grid spacing
 $\log g$ [cm/s²]: 4.0 $\leq \log g \leq$ 9.9
 Minimum 7.0 Maximum 7.0 Grid spacing 0.5

Abundances [mass fractions, preset with solar values (Asplund et al. 2009, ARAA 47, 481, Scott et al. 2015, A&A 573, A25)]:

H: 7.37E-01 He: 2.492E-01
 C: 2.365E-03 N: 6.928E-04 O: 5.733E-03
 Ne: 1.257E-03 Na: 2.923E-05 Mg: 7.079E-04

Presently, only SEDs of hot, compact stars can be calculated.
 This WWW interface is fully functional. The calculation of a H+He+C+N+O SED takes about one or two days, a H+He+C+N+O+Ne+Na+Mg SED calculation takes up to five days. Numerical instabilities may occur due to the requested parameters. We will then check for these asap.
 Please do not hesitate to start any calculation - this helps us to further improve the TMAW procedure.

Please do not hesitate to [contact us](#) should any question arise.

Figure B.5: TMAW homepage. Source: <http://astro.uni-tuebingen.de/~TMAW>, 27.01.2017

Model-Grid Parameters

T_{eff} [K]:	20 kK $\leq T_{\text{eff}} \leq$ 300 kK	
T_{eff} [K] (pure H+He):	20 kK $\leq T_{\text{eff}} \leq$ 1 MK	
Minimum	Maximum	Grid spacing
<input type="text" value="100000"/>	<input type="text" value="100000"/>	<input type="text" value="20000"/>
$\log g$ [cm/s ²]:	4.0 $\leq \log g \leq$ 9.9	
Minimum	Maximum	Grid spacing
<input type="text" value="7.0"/>	<input type="text" value="7.0"/>	<input type="text" value="0.5"/>

Abundances [mass fractions, preset with solar values ([Asplund et al. 2009, ARAA 47, 481](#); [Scott et al. 2015, A&A, 573, A25](#))]:

H: <input type="text" value="7.374E-01"/>	He: <input type="text" value="2.492E-01"/>	
C: <input type="text" value="2.365E-03"/>	N: <input type="text" value="6.928E-04"/>	O: <input type="text" value="5.733E-03"/>
Ne: <input type="text" value="1.257E-03"/>	Na: <input type="text" value="2.923E-05"/>	Mg: <input type="text" value="7.079E-04"/>

Figure B.6: TMAW input fields.

Source: <http://astro.uni-tuebingen.de/~TMAW>, 12.01.2017

TMAW Request Submission Confirmation

Request successfully submitted!

You should receive an e-mail notification within the next minutes!
If this is not the case, please ensure the entered e-mail address is correct.
The job with your parameters has entered our queuing system now and will be executed as soon as possible.

Date of Submission: 2017-01-28 11:11:51

Personal Information

Last Name: Yannick
First Name: Pfeifer
Institute: Institut für Astronomie und Astrophysik
E-Mail: yannick.pfeifer@astro.uni-tuebingen.de

SED-table Request

A standard SED table within 5 - 2000 Å as well as a table within 3500 - 7000 Å (resolution ≈ 0.1 Å) will be calculated.

Data Delivery

The data products of this request will be sent to you via e-mail as soon as the model has been calculated.

Figure B.7: Request confirmation in TMAW.

Source: <http://astro.uni-tuebingen.de/~TMAW>, 12.01.2017

Model-Grid Parameters

$T_{\text{eff}} / \text{K} = 100000 - 100000$ ($\Delta T_{\text{eff}} = 20000 \text{ K}$)

$\log(g / \text{cm/s}^2) = 7.0 - 7.0$ ($\Delta \log g = 0.5$)

element	mass fraction
H	7.374E-01
He	2.492E-01
C	2.365E-03
N	6.928E-04
O	5.733E-03
Ne	1.257E-03
Na	2.923E-05
Mg	7.079E-04

Figure B.8: Confirmation of the requested parameters in TMAW.

Source: <http://astro.uni-tuebingen.de/~TMAW>, 12.01.2017

GERMAN ASTROPHYSICAL
GAVO
VIRTUAL OBSERVATORY

German Astrophysical Virtual Observatory
TVIS - Tübingen Visualization Tool

Home

- About GAVO
- Getting Started
- GAVO Data Center
- Documents
- Internal

Login

(0.448 | 1.0323)

Plot box

Header

X_{Min} X_{Max}

Y_{Min} Y_{Max}

X Scientific notation Digits

Y Scientific notation Digits

Recticle

Datasets

Dataset 1 Dataset 3

Dataset 2 Dataset 4

Y_{Ident}

Default identifications

Y_{Ident}

Series 1 2 3 4 5 6

HI

He I

He II

System

Dataset 1: Keine ausgewählt

Dataset 2: Keine ausgewählt

Dataset 3: Keine ausgewählt

Dataset 4: Keine ausgewählt

Identification: Keine ausgewählt

When publishing research making use of this tool, please acknowledge:
 "The TVIS tool (<http://astro.uni-tuebingen.de/~TVIS/>) used for this paper was constructed as part of the activities of the German Astrophysical Virtual Observatory."

Sponsored by

Federal Ministry of Education and Research

Member of the International Virtual Observatory Alliance

Figure B.9: The TVIS Interactive Homepage.
 Source: <http://astro.uni-tuebingen.de/~TVIS/>, 12.01.2017

Please do not hesitate to [contact us](mailto:contact.us) should any question arise.

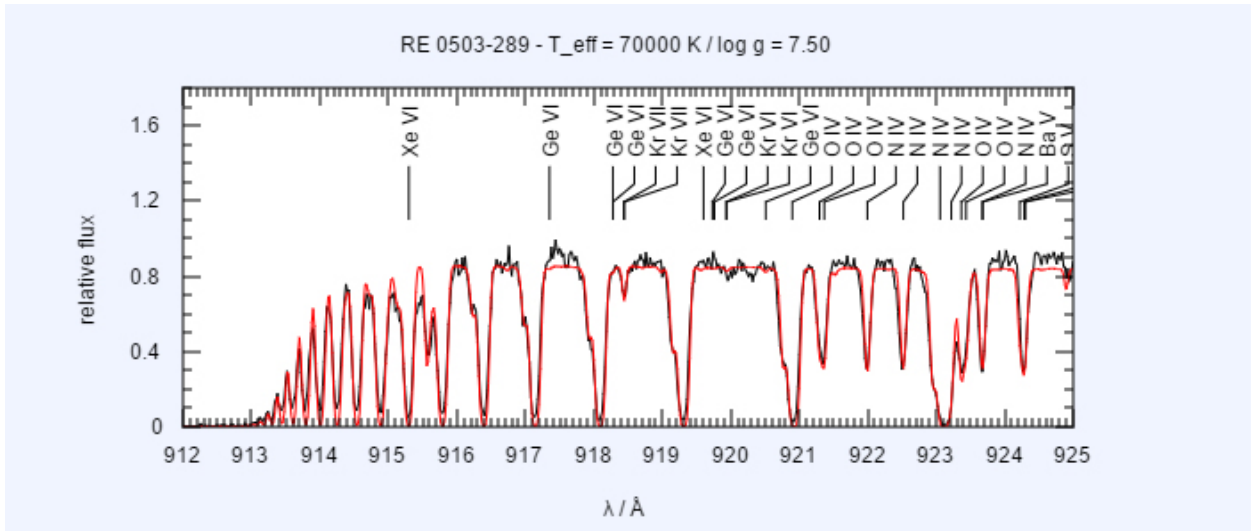


Figure B.10: Saveable image.

Source: <http://astro.uni-tuebingen.de/~TVIS>, 12.01.2017

In the framework of the Tübingen German Astrophysical Virtual Observatory (GAVO) project, we have developed the registered Tübingen Visualization tool (TVIS) that allows the user to plot data the easy way. The plotter itself is written in HTML5 and Javascript. To strongly increase the security of this web application, no Flash or Java is necessary to use it, i.e., TVIS will even work when Flash is dead and Java applets are blocked by the browsers.

How to use

There exist a variety of possibilities to use this application. The easiest way is the **<embed>** tag that calls the template of the first version (v1.0).

```
<embed width="<width>" height="<height>" src="http://astro.uni-tuebingen.de/~TVIS/tp/v1.0/index.html">
```

width and **height** represent the dimension of the embed object, not of the plot box. So, it makes more sense to set the dimension of the plot box and fit then the embed object. This can be achieved easily with the following.

```
<embed width="<width + 25>" height="<height + 25>" src="http://astro.uni-tuebingen.de/~TVIS/tp/v1.0/index.html?width=<width>&height=<height>">
```

To omit scrollbars, the embed object is 25 pixel in both directions larger than the plot box. Specific commands for the plotter have to be written in a plot config file. The user can commit it with the following line.

```
<embed width="<width + 25>" height="<height + 25>" src="http://astro.uni-tuebingen.de/~TVIS/tp/v1.0/index.html?width=<width>&height=<height>&config=<path>">
```

Keep in mind, that you should use **&** in the URL instead of **&**.

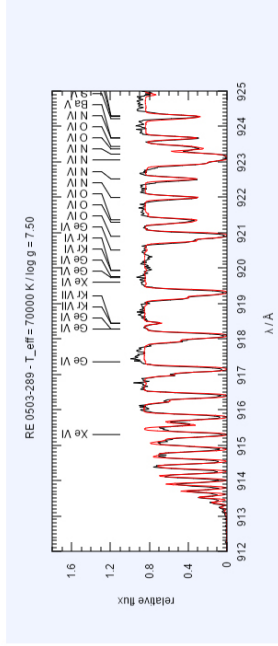
Commands

All commands that are available for the respective template and some examples can be found [here](#). If you feel that a useful command is missing, please let us know.

When publishing research making use of this tool, please acknowledge:

"The TVIS tool (<http://astro.uni-tuebingen.de/~TVIS/>) used for this paper was constructed as part of the activities of the German Astrophysical Virtual Observatory."

 **WEB**: This page was visited **96** times since August 02, 2016



TVISDataChanger

To improve the performance of TVIS, the user should only use data files that fit exactly the visible interval of the plot range. To modify an ensemble of data points, i.e., a spectrum, we have developed the TVISDataChanger. This small tool allows the user to cut, re-grid, and convolve (Gaussian or box profile) an ensemble of data points.

The tool is written in Java and can be downloaded [here](#).

Note: We have used the source code from www.java2s.com for the interpolation.

Objects

- [Ergas 110](#)
- [G101LB2B](#)
- [RC 0503-289](#)

Please do not hesitate to [contact](#) us should any question arise.

Figure B.11: TVIS homepage. Source: <http://astro.uni-tuebingen.de/~TVIS/>, 12.01.2017

How to use

There exist a variety of possibilities to use this application. The easiest way is the **<embed>** tag that calls the template of the first version (v1.0).

```
<embed width="<width>" height="<height>" src="http://astro.uni-tuebingen.de/~TVIS/tpl/v1.0/index.html">
```

width and **height** represent the dimension of the embed object, not of the plot box. So, it makes more sense to set the dimension of the plot box and fit then the embed object. This can be achieved easily with the following.

```
<embed width="<width + 25>" height="<height + 25>" src="http://astro.uni-tuebingen.de/~TVIS/tpl/v1.0/index.html?width=<width>&height=<height>">
```

To omit scrollbars, the embed object is 25 pixel in both directions larger than the plot box. Specific commands for the plotter have to be written in a plot config file. The user can commit it with the following line.

```
<embed width="<width + 25>" height="<height + 25>" src="http://astro.uni-tuebingen.de/~TVIS/tpl/v1.0/index.html?width=<width>&height=<height>&config=<path>">
```

Keep in mind, that you should use **&** in the URL instead of **&**.

Commands

All commands that are available for the respective template and some examples can be found [here](#). If you feel that a useful command is missing, please let us know.

Figure B.12: Instructions to embed the TVIS plotter in a homepage.

Source: <http://astro.uni-tuebingen.de/~TVIS>, 12.01.2017

Commands

All commands are not case sensitive. Colours must be given in HTML form. The name of the plots as well as all names within a plot must be unique. "" can be used in the config file as the comment sign.

The following commands are only for the template v1.0 (<http://astro.uni-tuebingen.de/~TVIS/tpl/v1.0/index.html>).

Figure B.13: Optional TVIS commands.

Source: <http://astro.uni-tuebingen.de/~TVIS/commands.shtml>, 12.01.2017

Parameters for the axis

Command	Description
\X-MIN <min>	Set the minimum of the x-axis
\X-MAX <max>	Set the maximum of the x-axis
\X-SPLITTING <splitting>	Set the separations of the ticks
\X-TICKLABEL <label>	Set the positions of the tick labels
\Y-MIN <min>	Set the minimum of the y-axis
\Y-MAX <max>	Set the maximum of the y-axis
\Y-SPLITTING <splitting>	Set the separations of the ticks
\Y-TICKLABEL <label>	Set the positions of the tick labels
\X-SCROLLABLE <true false>	Should the plot box be scrollable? Default: false
\X-SCROLLINTERVAL <interval>	Set the displayed interval of the x-axis
\X-SCROLLSTEP <splitting>	Set the scroll velocity of the x-axis for the mouse wheel
\X-TICK-BOTTOM <true false>	Do you want to see the ticks at the bottom? Default: true
\X-TICK-TOP <true false>	Do you want to see the ticks at the top? Default: true
\X-TICK-LEGEND <true false>	Do you want to see the labels of the ticks? Default: true
\Y-TICK-LEFT <true false>	Do you want to see the ticks at the bottom? Default: true
\Y-TICK-RIGHT <true false>	Do you want to see the ticks at the top? Default: true
\Y-TICK-LEGEND <true false>	Do you want to see the labels of the ticks? Default: true
\TICK-LENGTH-SMALL <length>	Set the length of the small tick
\TICK-LENGTH-LARGE <length>	Set the length of the large tick

Object (data points)

"" can be used in the data file as the comment sign.

Command	Description
\OBJECT LOAD <name> <url> <x-column> <y-column> [grid]	Loads a x-y-table from a specific URL The grid parameter is optional
\OBJECT COLOUR <name> <colour>	Set the colour of the object
\OBJECT CALC <name> X+ <number>	Add a number to all x-values
\OBJECT CALC <name> X- <number>	Subtract a number of all x-values
\OBJECT CALC <name> X* <number>	Multiply all x-values by a number
\OBJECT CALC <name> X/ <number>	Divide all x-values by a number
\OBJECT CALC <name> XLOG <number>	Take the logarithm of all x-values
\OBJECT CALC <name> XDEX <number>	Withdraw the logarithm of all x-values
\OBJECT CALC <name> Y+ <number>	Add a number to all y-values
\OBJECT CALC <name> Y- <number>	Subtract a number of all y-values
\OBJECT CALC <name> Y* <number>	Multiply all y-values by a number
\OBJECT CALC <name> Y/ <number>	Divide all y-values by a number
\OBJECT CALC <name> YLOG <number>	Take the logarithm of all y-values
\OBJECT CALC <name> YDEX <number>	Withdraw the logarithm of all y-values

Figure B.13: Continuation.

Main Command

Command	Description
\Plot <name>	Every plot has to start with this and all commands till to the next \PLOT command describe a plot unit.

Plotter layout

Command	Description
\OUTER-BACKGROUND-COLOUR <colour>	Set the colour of the background
\INNER-BACKGROUND-COLOUR <colour>	Set the colour of the plot box
\PLOTBOX-COLOUR <colour>	Set the edge colour of the plot box
\FONTSIZE <size>	Set the font size
\FONT-COLOUR <colour>	Set the font colour
\HEADER <header>	Set the header
\X-AXIS-LEGEND <legend>	Set the lable of the x-axis
\Y-AXIS-LEGEND <legend>	Set the lable of the y-axis

Figure B.13: Continuation.

Identification

The identifications in a file must have the following syntax: <wavelength|x-position> <name>

Command	Description
\IDENT LOAD <name> <url>	Loads all identifications from a specific file
\IDENT COLOUR <name> <colour>	Set the colour of the identifications
\IDENT Y-POS <name> <y-pos>	Set the y-position (in units) of the identifications

Figure B.13: Continuation.

TVISDataChanger

To improve the performance of TVIS, the user should only use data files that fit exactly the visible interval of the plot range. To modify an ensemble of data points, i.e., a spectrum, we have developed the TVISDataChanger. This small tool allows the user to cut, re-grid, and convole (Gaussian or box profile) an ensemble of data points.

The tool is written in Java and can be downloaded [here](#).

Note: We have used the source code from www.java2s.com for the interpolation.

Figure B.14: The TVIS Data Changer.

Source: <http://astro.uni-tuebingen.de/~TVIS>, 12.01.2017

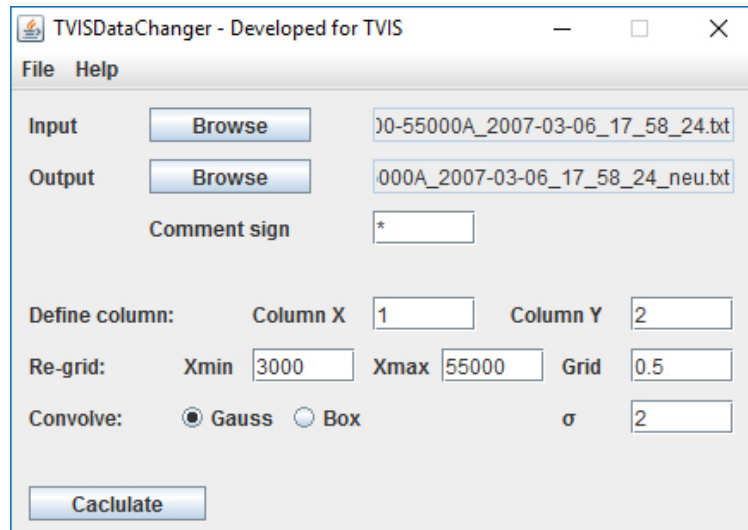


Figure B.15: TVIS Data Changer opened in a window.

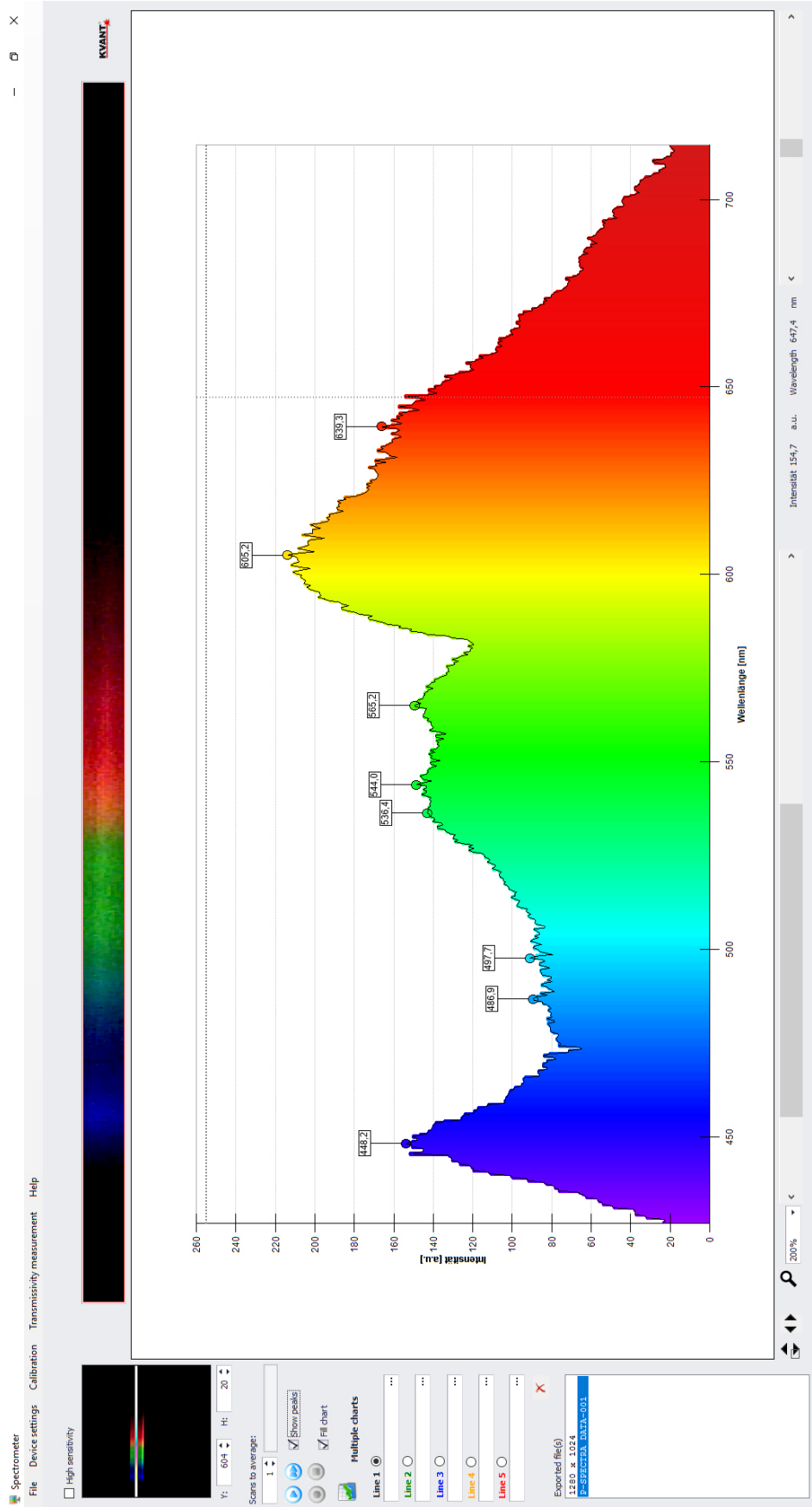


Figure B.16: The SPECTRA 1 user interface.

C Datasets

C.1 TMAW Output

Example of the beginning of a synthetic spectra file from TMAW.

```
* TUEBINGEN NLTE MODEL ATMOSPHERE PACKAGE (TMAP)
* http://astro.uni-tuebingen.de/~TMAP
*
* References:
*
* Werner K., et al. 2003,
*   Model Photospheres with Accelerated Lambda Iteration,
*   in: Workshop on Stellar Atmosphere Modeling,
*   eds. I. Hubeny, D. Mihalas, K. Werner,
*   The ASP Conference Series Vol. 288 (San Francisco: ASP), p. 31
* Rauch T., Deetjen J. L. 2003,
*   Handling of Atomic Data,
*   in: Workshop on Stellar Atmosphere Modeling,
*   eds. I. Hubeny, D. Mihalas, K. Werner,
*   The ASP Conference Series Vol. 288 (San Francisco: ASP), p. 103
*
* please do not hesitate to contact
* astro-tmap@listserv.uni-tuebingen.de for further information
*
*
* DATA FILE CREATED BY LINE1 AT 02-03-16 15:39:23
* MODEL CALCULATED BY PRO2 AT 12-02-16 11:50:51
*
* T eff = 100000 K
* log g = 7.00 (cgs)
*
* NORMALIZED MASS FRACTIONS
*
* H 1.000E+00
*
* COLUMN 1: WAVELENGTH GIVEN IN A
*           (VACUUM WAVELENGTHS FOR LAMBDA < 3000 A)
* COLUMN 2: F LAMBDA GIVEN IN ERG/CM**2/SEC/CM
* COLUMN 3: RELATIVE FLUX (F LINE / F CONT)
* -----
* 12499 LINES FOLLOWING
9.10500000E+02 1.888582E+19 1.000000
9.11000000E+02 1.885533E+19 1.000000
9.11500000E+02 1.882487E+19 1.000000
9.11753463E+02 1.880946E+19 1.000000
```

C.2 TVIS Data Changer Output

Example of a synthetic spectra file after it has been edited by the TVIS Data Changer.

```
915.00000 9.998870E-01
917.00000 9.996110E-01
919.00000 9.959440E-01
921.00000 5.848450E-01
923.00000 5.258590E-01
925.00000 8.856800E-01
927.00000 7.331150E-01
929.00000 9.149190E-01
931.00000 4.416750E-01
933.00000 9.472440E-01
935.00000 9.586250E-01
937.00000 6.693150E-01
939.00000 7.819350E-01
941.00000 9.721560E-01
943.00000 9.896130E-01
945.00000 9.860170E-01
947.00000 9.462570E-01
949.00000 6.392190E-01
951.00000 7.854250E-01
953.00000 9.653230E-01
955.00000 9.907990E-01
957.00000 9.957190E-01
959.00000 9.968670E-01
961.00000 9.967930E-01
963.00000 9.957690E-01
965.00000 9.931320E-01
967.00000 9.861750E-01
969.00000 9.623630E-01
971.00000 8.320470E-01
973.00000 5.294770E-01
975.00000 9.231930E-01
977.00000 9.781200E-01
979.00000 9.908230E-01
981.00000 9.952200E-01
983.00000 9.971230E-01
985.00000 9.980930E-01
987.00000 9.986360E-01
989.00000 9.989580E-01
991.00000 9.991590E-01
```

C.3 Spectra 1 Output

Beispiel für eine Ausgabedatei von Spectra-1:

Spectrometer

Copyright Kvant 2014. All rights reserved.

Datum:Freitag, 10. Februar 2017 16:24:51

Name des Quellbildes:.bmp

Quellbild [pixel]:1280 x 1024

Bearbeitete Hohe des Quellbildes [Pixel]:20

Bearbeitetes Quellbild [Position Pixel Bereich]:604 - 624

Spektrumbereich [nm]:360.1 - 934.9

Diagrammpunkte:

Wellenlänge [nm] Intensitat [a.u]

===START===

360.1	0.0
360.5	0.0
361.0	0.0
361.4	0.0
361.9	0.0
362.3	0.0
362.8	0.0
363.2	0.0
363.7	0.0
364.1	0.0
364.6	0.0
365.0	0.0
365.5	0.0
365.9	0.0
366.4	0.0
366.8	0.0
367.3	0.0
367.7	0.0
368.2	0.0
368.6	0.0
369.1	0.0
369.5	0.0
370.0	0.0
370.4	0.0

D Declaration to the scientific paper

Ich erkläre, dass ich die Arbeit selbständig angefertigt und nur die angegebenen Hilfsmittel benutzt habe. Alle Stellen, die dem Wortlaut oder dem Sinn nach anderen Werken, gegebenenfalls auch elektronischen Medien, entnommen sind, sind von mir durch Angabe der Quelle als Entlehnung kenntlich gemacht. Entlehnungen aus dem Internet sind durch Angabe der Quelle und des Zugriffsdatums sowie dem Ausdruck der ersten Seite belegt; sie liegen zudem für den Zeitraum von zwei Jahren entweder auf einem elektronischen Speichermedium im PDF-Format oder in gedruckter Form vor.

Datum

Unterschrift